Phosphoproteomics to Characterize Host Response During Influenza A Virus Infection of Human Macrophages*[S]

Sandra Söderholm‡§, Denis E. Kainov¶, Tiina Öhman‡, Oxana V. Denisova¶, Bert Schepens‖, Evgeny Kulesskiy¶, Susumu Y. Imanishi‡‡[a], Garry Corthals‡‡[b], Petteri Hintsanen¶, Tero Aittokallio¶, Xavier Saelens‖**, Sampsa Matikainen§§[c], and Tuula A. Nyman‡¶¶[c]‖‖**

Influenza A viruses cause infections in the human respiratory tract and give rise to annual seasonal outbreaks, as well as more rarely dreaded pandemics. Influenza A viruses become quickly resistant to the virus-directed antiviral treatments, which are the current main treatment options. A promising alternative approach is to target host cell factors that are exploited by influenza viruses. To this end, we characterized the phosphoproteome of influenza A virus infected primary human macrophages to elucidate the intracellular signaling pathways and critical host factors activated upon influenza infection. We identified 1675 phosphoproteins, 4004 phosphopeptides and 4146 nonredundant phosphosites. The phosphorylation of 1113 proteins (66%) was regulated upon infection, highlighting the importance of such global phosphoproteomic profiling in primary cells. Notably, 285 of the identified phosphorylation sites have not been previously described in publicly available phosphorylation databases, despite many published large-scale phosphoproteome studies using human and mouse cell lines. Systematic bioinformatics analysis of the phosphoproteome data indicated that the phosphorylation of proteins involved in the ubiquitin/proteasome pathway (such as TRIM22 and TRIM25) and antiviral responses (such as MAVS) changed in infected macrophages. Proteins known to play roles in small GTPase–, mitogen-activated protein kinase–, and cyclin-dependent kinase- signaling were also regulated by phosphorylation upon infection. In particular, the influenza infection had a major influence on the phosphorylation profiles of a large number of cyclin-dependent kinase substrates. Functional studies using cyclin-dependent kinase inhibitors showed that the cyclin-dependent kinase activity is required for efficient viral replication and for activation of the host antiviral responses. In addition, we show that cyclin-dependent kinase inhibitors protect IAV-infected mice from death. In conclusion, we provide the first comprehensive phosphoproteome characterization of influenza A virus infection in primary human macrophages, and provide evidence that cyclin-dependent kinases represent potential therapeutic targets for more effective treatment of influenza infections. ***Molecular & Cellular Proteomics 15: 10.1074/mcp.M116.057984, 3203–3219, 2016.***

Influenza A viruses (IAVs)[1] cause annual epidemics and occasionally worldwide pandemics, infecting millions of people. IAVs are negative-stranded RNA viruses belonging to *Orthomyxoviridae* family. The options to control the spread of human influenza are vaccination and antivirals. The current antiviral drugs used for treatment of IAV infections target the viral proteins. The influenza viruses mutate rapidly to escape host immune responses developed after previous infection or vaccinations (1) and these high mutation rates lower the effi-

From the ‡Institute of Biotechnology, FI-00014 University of Helsinki, Helsinki, Finland; §Unit of Systems Toxicology, Finnish Institute of Occupational Health, FI-00250 Helsinki, Finland; ¶Institute for Molecular Medicine Finland (FIMM), FI-00014 University of Helsinki, Helsinki, Finland; ‖Medical Biotechnology Center, VIB, B-9052 Ghent (Zwijnaarde), Belgium; **Department of Biomedical Molecular Biology, B-9052 Ghent University, Ghent, Belgium; ‡‡Turku Centre for Biotechnology, University of Turku and Åbo Akademi University, FI-20520 Turku, Finland; §§Department of Rheumatology, University of Helsinki and Helsinki University Hospital, Helsinki, Finland; ¶¶Institute of Clinical Medicine, University of Oslo, Norway

Received January 9, 2016, and in revised form, July 19, 2016
Published, MCP Papers in Press, August 2, 2016, DOI 10.1074/mcp.M116.057984
Author contributions: D.E.K., X.S., S.M., and T.A.N. designed research; S.S., D.E.K., T.O., O.V.D., B.S., E.K., S.Y.I., and P.H. performed research; G.C., T.A., and X.S. contributed new reagents or analytic tools; S.S., D.E.K., T.O., O.V.D., B.S., X.S., S.M., and T.A.N. analyzed data; S.S., D.E.K., S.M., and T.A.N. wrote the paper.

[1] The abbreviations used are: CDK, cyclin-dependent kinase; CDKI, cyclin-dependent kinase inhibitor; GM-CSF, granulocyte-macrophage colony-stimulating factor; GSK3B, glycogen synthase kinase beta; IAV, influenza A virus; IFN, interferon; IPA, Ingenuity Pathway Analysis; IRF3, interferon regulatory factor 3; KEA, kinase enrichment analysis; MAPK, mitogen-activated protein kinase; MAVS, mitochondrial antiviral signalling protein; NF-κB, nuclear factor kappa-light-chain-enhancer of activated B cells; NS1, nonstructural protein 1; NP, nucleoprotein; PKA, cAMP-dependent protein kinase; PKC, protein kinase C; RIG-I, retinoic acid-inducible gene 1; ROCK2, Rho-associated coiled-coil containing protein kinase 2; TNF, tumor necrosis factor.

cacy of antiviral treatment that target viral proteins (2, 3). To address the resistance problem, it is crucial to find novel noncytotoxic drugs targeting conserved virus-host interactions, which are critical for IAV infection and replication. Inhibiting such interactions provide improved opportunities to reduce the occurrence of drug-resistant mutants and to minimize the morbidity and mortality caused by IAVs.

The host response to pathogens is complex and dynamic. Proteomics can shed light on this response and provide the system-level information of the immune response required for detailed understanding of disease mechanisms (4, 5). Mass spectrometry (MS)-based proteomics has become a powerful tool for analyzing protein abundances, modifications and interactions. The current MS technology allows identification, quantification, and characterization of post-translational modifications of thousands of proteins in a single experiment. In biomedicine, phosphoproteins are intriguing candidates for therapeutic interventions because the upstream kinases are relatively easy to target selectively with small molecule drugs (6). Previous MS-based phosphoproteome studies have shown major effects on host protein phosphorylation and reorganization of signal-transduction pathways in viral infections such as HIV-1 (7), lytic γ herpesvirus infection (8), porcine reproductive and respiratory syndrome virus (9), rift valley virus (10), Sendai virus (11), and human cytomegalovirus (12) infections.

Macrophages are professional phagocytes and one of the first cells to encounter pathogens in tissues. Macrophages often reside in or are recruited to infection sites, and they are important generators of inflammatory responses (13). Macrophages are also one of the most abundant phagocytes in the respiratory tract tissue and lung, and they are therefore thought to play a key role in the control and clearance of IAV infections (14). We previously published a subcellular proteome and secretome characterization of IAV infected primary human macrophages, which demonstrated that viral infection perturbs the expression and subcellular localization of more than a thousand host proteins at early phases of infection (15). Here, we have characterized the phosphoproteome of IAV infected human macrophages in order to identify the host kinases and their substrates that play a critical role in the early stages of infection. We identified 1675 human phosphoproteins and in total 1113 proteins showed changes in their phosphorylation status upon IAV infection, implying that the IAV infection has a profound effect on host protein phosphorylation. These host proteins are involved in all critical stages of virus life cycle including viral entry, gene regulation, and egress. The data also showed that IAV infection influences the phosphorylation status of several cyclin-dependent kinases (CDKs) and their substrates. Functional studies showed that the CDK activity is required for efficient viral replication and for the activation of antiviral and pro-inflammatory responses.

EXPERIMENTAL PROCEDURES

Ethics Statement—All mouse experiments were conducted in strict accordance with national (Belgian Law 14/08/1986 and 22/12/2003, Belgian Royal Decree 06/04/2010) and European (EU Directives 2010/63/EU, 86/609/EEG) animal regulations. Animal protocols were approved by the ethics committee of Ghent University (permit number LA1400091, approval ID 2010/001). All human blood donors provided written informed consent.

Cells and Cell Stimulation—Primary human macrophages were derived from leukocyte-rich buffy coats from healthy blood donors (Finnish Red Cross Blood Transfusion Service, Helsinki, Finland). Monocytes were isolated and differentiated into macrophages as described previously (16). In total 1.4×10^6 monocytes were seeded per well on 6-well plates or 5×10^4 per well on 96-well plates. The monocytes were cultured in serum free macrophage media (Gibco®, Thermo Fisher Scientific, Waltham, MA) supplemented with 10 ng/ml granulocyte-macrophage colony-stimulating factor (GM-CSF) (BIOSOURCE International, Thermo Fisher Scientific) and 50 U/ml penicillin-streptomycin (Lonza, Basel, Switzerland) at 37 °C and 5% CO_2 for 7 days, polarizing the monocytes into macrophages of the acute pro-inflammatory M1-phenotype. Before stimulation, the media was replaced with fresh GM-CSF free macrophage media and macrophages were infected with influenza A virus. MDCK cells (Sigma-Aldrich, St Louis, MO, catalog number 8412190) were maintained at 37 °C and 5% CO_2 in DMEM (Sigma-Aldrich) supplemented with 10% fetal bovine serum (Gibco®, Thermo Fisher Scientific), 2 mM L-glutamine (Lonza), and 50 U/ml penicillin-streptomycin (Lonza).

Virus Stocks and Infections—Human pathogenic influenza A/Udorn/307/1972 (H3N2), provided by the National Institute for Health and Welfare, was cultured in embryonated hen eggs and the virus stock, with a titer of 256 hemagglutination U/ml, was stored at −80 °C. A virus dose of 2.56 hemagglutination U/ml was used in the infection experiments unless stated otherwise. The virus experiments were carried out under BSL-2 conditions and in compliance with regulations of the University of Helsinki (permit No 21/M/09). The mice studies were conducted with a mouse-adapted influenza A virus, H1N1 A/Puerto Rico/8/34 (PR8) (17), obtained as a kind gift from Dr. Skehel. The PR8 virus was adapted to mice by serial lung passage and propagated in MDCK cells in the presence of TPCK-treated trypsin.

Phosphoproteomics and Bioinformatics—Macrophages grown on six-well plates were used for the phosphoproteomics experiments. The cell growth media was changed to GM-CSF free growth media (1 ml/well) one hour before infection with a virus dose of 2.56 hemagglutination U/ml. The macrophages were left untreated (control) or infected with IAV for 6 h. The cell media was removed and the cells were washed with PBS, and then incubated in PBS on ice for 5 min, after which they were scraped off with a rubber policeman. The cell solution was centrifuged $404 \times g$ for 5 min. The supernatant was removed and the cell pellet was re-suspended in 10 ml of ice-cold PBS and the centrifugation step was repeated. The cells were lysed with HEPES lysis buffer (50 mM HEPES, 150 mM NaCl, 1 mM EDTA, 1% Nonidet P-40, pH 7.4, including protease and phosphatase inhibitor cocktails from Sigma-Aldrich), the lysates were centrifuged, and the protein content was measured with Bio-Rad DC™ (Bio-Rad Laboratories, Hercules, CA). The digestion of the proteins in the cell lysates (10 mg per sample), the clean-up, desalting steps, strong cation exchange fractionation, and phosphopeptide enrichment with IMAC were performed as described previously (18). The LC-MS/MS analysis was done with a Q Exactive ESI-quadrupole-orbitrap mass spectrometer coupled to an EASY-nLC 1000 nanoflow LC (Thermo Fisher Scientific) as described previously (19). Two biological replicates were analyzed (in total two control and two IAV infected sam-

ples), both replicates including equal amounts of cells from four different donors.

Raw files were processed in the Proteome Discoverer interface (version 1.3, Thermo Fisher Scientific, SanJose, CA) and the MS/MS spectra were searched using the Mascot algorithm (Matrix Science, version 2.4.0) against a concatenated forward-reverse SwissProt database (release date April 2012, *Homo sapiens*) supplemented with common contaminants (total of 40,678 protein sequences) to identify human proteins. To identify IAV proteins, the LC-MS/MS data was searched against a SwissProt database with IAV and human protein sequences (version 02/2012, total of 21,545 sequences). Search parameters included tryptic specificity with allowance of maximum two missed cleavage sites. The peptide charge was specified as 2+ and 3+, the precursor mass tolerance as 5 ppm, and the MS/MS ion tolerance as 0.02 Da. Carbamidomethylation (C) was specified as fixed modification, and oxidation (M), phosphorylation (S, T, and Y) and acetylation (protein N-terminal) as variable modifications. The mass spectrometry proteomics data have been deposited to the ProteomeXchange Consortium (20) via the PRIDE partner repository with the data set identifier PXD001620.

The peptide spectra matches (PSMs) were filtered with a false discovery rate (FDR) of 1% in Proteome Discoverer applying the Percolator algorithm. Other thresholds applied were: maximum peptide rank, 1; peptides per protein, minimum 1, count only rank 1 peptides. The phosphoRS algorithm (21) was applied to assign localization scores for the identified phosphorylation sites. The PSMs of phosphopeptides with Mascot ion score $\geq$ 30 (peptide FDR $<$ 1%) were selected and exported from Proteome Discoverer for further analysis with the in-house developed phosphoproteomic data analysis tool, PhosFox (22). The results from two biological replicates were combined when performing the PhosFox analysis. In addition, PhosFox considered a phosphopeptide with different number of missed cleavages as single phosphopeptide. A phosphopeptide was considered "unique" to a sample if PhosFox detected it only in one sample (*e.g.* infected), but not in the other sample (*e.g.* control). The proteins with phosphopeptides that were unique to control and infected samples were chosen for bioinformatics analyses. Pathway analysis and classification of proteins based on gene ontology annotations were carried out with Ingenuity Pathway Analysis (IPA) (Qiagen, Hilden, Germany) and InnateDB database (23). The NetworKIN algorithm (24) in KinomeXplorer was used for predicting kinases associated with specified phosphosites and Kinase Enrichment Analysis (KEA) (25) for identifying kinase substrates in the phosphoproteomic data.

Compound Efficacy Testing In Vitro and Virus Titration—SNS-032, flavopiridol, dinaciclib, roscovitine, and pablociclib (all from Selleckchem, Houston, TX) were dissolved in DMSO (Sigma-Aldrich) to 10 mM stock solutions and stored at −80 °C. DMSO was used as control in the experiments. The compound efficacy testing was performed in 96-well plates with macrophages at 95% confluence. The compounds were added to the medium and one hour later the cells were infected with virus or noninfected (mock). The cell viability was analyzed with the Cell Titer Glo assay (CTG; Promega, Madison, WI) at 24 h post-infection. The luminescence was read with a PHERAstar FS plate reader (BMG Labtech, Thermo Fisher Scientific).

The 50% cytotoxic concentration (CC_{50}) of cyclin-dependent kinase inhibitor (CDKI) treatment was determined with the CTG assay in macrophages treated with different concentrations of CDKI (0 to 20 μM) for 24 h. The antiviral effect, the half maximal effective concentration (EC_{50}) of the inhibitor, *i.e.* the ability of the inhibitor to reduce virus production to 50%, was calculated by measuring the titers of viruses grown in macrophages (initial MOI 0.01) for 24 h in the presence of 0 to 20 μM CDKI. The selectivity index (SI) was defined as the CC_{50}/EC_{50} ratio.

The antiviral efficacies of the CDKIs were validated by the plaque assay as described previously (26). The macrophages were non- or compound-treated and infected with IAV (MOI of 0.01). The virus titers were determined by calculating the plaque forming units (PFU) (clear spots) for each sample and expressed as PFU/ml.

Western Blotting—Equal amounts of protein from total cell lysis samples were dissolved in Laemmli buffer and resolved by SDS-PAGE (Bio-Rad). The proteins were transferred onto Immobilon-P membranes (Millipore, Billerica, MA). The membranes were blocked with 5% nonfat milk or 5% BSA (Sigma-Aldrich) in TBST, stained with different primary antibodies overnight, followed by secondary antibody labeling and detection by the ImageQuant LAS 4000 mini Luminescent Image Analyzer (GE Healthcare, Little Chalfont, UK). The primary antibodies used in this study were anti-phospho(Ser396)-IRF3 (4D4G) (Cell Signaling, Danvers, MA, #4947), anti-IRF3 (FL-425) (Santa Cruz, Heidelberg, Germany, sc-9082), anti-IκBα (44D4) (Cell Signaling, #4812), anti-Bcl-X_L (Santa Cruz, sc-56021), anti-cleaved caspase 3 (Asp175) (Cell Signaling #9661). These antibodies were diluted 1:1000 in 5% BSA-TBST or in 5% milk-PBST (the IRF3 antibody). Anti-IAV (H3N2) NS1 and NP antibodies (1:5000 dilution in 5% BSA-TBST) have been previously described (16, 27). To confirm equal sample loading the membranes were stripped and labeled with anti-GAPDH (0411) (Santa Cruz, sc-47724), 1:1000 dilution in 5% milk-PBST.

RT-PCR—Total cellular RNA was isolated with the RNeasy Plus Mini Kit (Qiagen) and the RNA was reverse transcribed using the High Capacity cDNA Reverse Transcription kit (Applied Biosystems, Carlsbad, CA), according to the manufacturer's instructions. RT-qPCR was run with an ABI PRISM 7500 Sequence Detection System, applying TaqMan chemistry and Predeveloped TaqMan assay primers and probes (Applied Biosystems) and TaqMan® Fast Advanced Master Mix (Applied Biosystems). The following TaqMan probes were used: 18S: Hs99999901_s1, IFN-β: Hs01077958_s1, and IL-29 (IFN-λ1): Hs00601677_g1, CXCL10 (IP-10): Hs01124251_g1, CXCL11 (I-TAC): Hs04187682_g1. Human GAPDH (forward primer: ggctggggctcatttgcaggg and reverse primer: tgaccttggccaggggtgct) from (Oligomer Oy, Helsinki, Finland) and Influenza A (H3N2) virus primers detecting PB1 (PB1_5pr forward primer: ccaaactggcaaatgttgtg and PB1_5pr reverse primer: tgcgatgctcagaatgtttc) from Dr. Ville Veckman, M2 (forward primer: aagaccaatcctgtcacctctga and reverse primer: caaaggcgtctacgctgcagtcc) and NP (forward primer: accaggagtggaggaaacacta and reverse primer: ttcaaatgggaggtttctctgt) from Prof. Ilkka Julkunen, were used with SYBR Green Master Mix (Applied Biosystems).

The sequence detector system software version 4.1 was used for the collection of real-time PCR data. The relative gene expression differences were calculated with the comparative $\Delta\Delta$Ct method as described before (28). The results are represented as relative units (RU). Each sample was analyzed in duplicate or triplicate on the same qPCR plate and nontemplate samples and a nonreverse transcriptase samples were analyzed routinely as negative controls.

Cytokine Profiling, Luminex Assay and Caspase Activation Assay—The cytokine arrays Proteome Profiler Human Cytokine Array Panel A kit (R&D Systems, Minneapolis, MN) were used for profiling cytokines according to the manufacturer's instructions. For the human macrophage *in vitro* experiments, the concentration of SNS-032 and flavopiridol was 0.3 μM and the cell culture supernatants were collected after 20 h of stimulation. The membranes were exposed to x-ray films and the films were scanned, or the chemiluminescence was measured with ImageQuant LAS 4000 mini (GE Healthcare, Uppsala, Sweden) and the fold change was calculated in comparison to the mock sample. The images were analyzed with ImageJ software (NIH).

For Luminex assay, primary human macrophages were pretreated with SNS-032 and flavopiridol (0.3 μM) or left untreated and infected with IAV or mock. The cell growth media were collected after 18 h of stimulation and centrifuged. The human cytokine Luminex Bio-Plex

Pro immunoassay (Bio-Rad Laboratories) designed to detect chemokines TNF, IL-1β, IL-1α, and IL-18 was performed according to the manufacturer's instructions using the Bio-Plex 200 system hardware and version 4.1.1 of the Bio-Plex 200 software.

Caspase 3/7, 8 and 9 activities in infected or noninfected macrophages, nontreated or treated with SNS-032 or flavopiridol at 0.3 μM, were measured with the Caspase-Glo-3/7, -8 and -9 assays (Promega) at 18 h. The Caspase-Glo® 1 Inflammasome assay (Promega) was used to measure the caspase 1 activity in infected or noninfected macrophages, nontreated or treated with SNS-032 at 0.3 μM at 18 h postinfected.

In Vivo Experiments—Pathogen-free 7-week-old female BALB/c mice were purchased form Charles Rivers Laboratories (Italy). The animals were housed in a SPF temperature-controlled environment with 12 h light/dark cycles and given water and food *ad libitum*. After 1-week adaptation in the animal room, six mice per group were treated with SNS-032 (15 mg/kg in 5% DMSO in 200 μl PBS) or vehicle (5% DMSO in 200 μl PBS) IP at 1 day before and 1, 3, 5, 7, and 9 days after infection. At day 0 the mice were sedated with isoflurane and challenged intranasally with 0.5 LD_{50} of mouse-adapted PR8. Body weight was monitored daily and mice that had lost more than 25% of their initial body weight were euthanized by cervical dislocation. The survival data of the mouse experiments were analyzed using SigmaStat 11.0 and the Log-rank (Mantel-Cox) test. The bodyweight changes were analyzed by two-way ANOVA test with Bonferroni's multiple comparison adjustment.

In the follow-up experiment, four mice per group were treated with SNS-032 (15 mg/kg in 5% DMSO in 200 μl PBS) or vehicle (5% DMSO in 200 μl PBS) IP at 1 day prior infection and 1 and 3 days after infection. At day 0 the mice were sedated with isoflurane and challenged intranasally with 0.5 LD_{50} of mouse-adapted PR8 or mock infected. Mice were sacrificed at 5 days post infection and the lung were collected and homogenized in 1.5 ml of PBS using a Heidolph RZR 2020 homogenizer. The homogenate was cleared using centrifugation at 1000 $\times$ *g* for 15 min at 4 °C. In total 200 μl of lung homogenates from four groups (noninfected/DMSO-treated, noninfected/SNS-032-treated, infected/DMSO-treated, and infected/SNS-032-treated) of four mice each were combined and assayed for cytokines with the Mouse cytokine array panel A (R&D Systems).

Mouse influenza virus infection experiments were carried out under BSL-2+ conditions and were authorised by the Institutional Ethics Committee on Experimental Animals of the Department for Medical Molecular Biology at Ghent University.

Experimental Design and Statistical Rationale—Data are shown as mean values and error bars represent standard deviation (S.D.) from the number of independent assays indicated in the figure legends. For two-group comparisons, a two-tailed unpaired *t* test was applied using Prism software (Graph-Pad Software, Inc.). The significance level is indicated as ****$p < 0.0001$; ***$p < 0.001$; **$p < 0.01$; *$p < 0.05$; $p > 0.05$ not significant (ns).

With phosphoproteomics, two independent biological replicate experiments were performed and the results from the replicates were combined when analyzing the data with the PhosFox software (22). See subsection Phosphoproteomics and Bioinformatics for more details.

RESULTS AND DISCUSSION

Phosphoproteome Analysis Shows Major Changes in Host Protein Phosphorylation After Influenza A Virus Infection of Human Macrophages—In order to get an integrated view of phosphorylation-regulated host proteins and signaling pathways by IAV infection in human macrophages, we used high resolution MS-based phosphoproteome analysis of control and infected samples combined with bioinformatics and functional assays. First, we studied the kinetics of viral replication and host response of human macrophages infected with influenza A/Udorn/307/1972 (H3N2) virus. The expression of viral mRNAs coding for matrix protein 2 (*M2*), nucleoprotein (*NP*), and RNA polymerase subunit 1 (*PB1*) was initiated at 4 h postinfection (supplemental Fig. S1). In accordance with the mRNA expression data, Western blot analysis demonstrated that viral proteins NP and nonstructural protein 1 (NS1) became detectable at 5–6 h after IAV infection (Fig 1*A*). Expression of antiviral cytokines *IFN-β1* and *IL-29 (IFN-λ1)* mRNA started already 1–2 h after infection, reaching high levels of expression at 6 h postinfection (supplemental Fig. S1).

The IRF3 and NF-kB signaling pathways are activated during viral infection leading to the expression of inflammatory genes including type I (IFN-α/β) and III interferons (IL-28 and IL-29), proinflammatory cytokines, and chemokines (29, 30). The IRF3 signaling pathway is also involved in the activation of apoptosis during viral infections (31, 32). To study the activation of these transcription factors during IAV infection, we performed Western blot analyses to probe for phosphorylation of IRF3 and degradation of IκBα, an inhibitor of NF-κB. Phosphorylation of IRF3 was weakly initiated at 2 h postinfection and strong activation of IRF3 was seen after 6 h of infection (Fig 1*A*). No change in the total amount of IRF3 was detected during the infection progression. Degradation of IκBα was first seen at 2 h after IAV infection and at 6 h postinfection IκBα was barely detectable, indicating the activation of NF-κB. These results demonstrate that there is a weak activation of IRF3 and NF-κB pathways at early stages of infection, 1–2 h after viral entry. This is followed by a robust activation of these signaling pathways at 6 h after infection, which correlates with the initiation of viral RNA transcription and translation.

Based on these experiments, we chose an infection time point of 6 h for the high resolution MS-based phosphoproteomics analysis (Fig 1*B*). Control and IAV-infected macrophages were lysed and the protein samples were digested into peptides followed by peptide fractionation and phosphopeptide enrichment before LC-MS/MS analysis of the peptides. For phosphoprotein and -peptide identification, the LC-MS/MS data was first processed with the Mascot search engine, and the final list of phosphopeptides was generated using an in-house-developed data analysis tool, PhosFox (22). We analyzed two independent biological replicates, which led to the identification of 4004 phosphopeptides and 4146 nonredundant phosphorylation sites, originating from 1675 different human phosphoproteins (Fig 1*C*, supplemental Tables S1 and S2). In total, 1113 human proteins showed qualitative changes in their phosphorylation profiles upon infection (Fig 1*C*), meaning that specific Y/S/T sites were identified as phosphorylated only in control sample or after infection (supplemental Table S3). Approximately 30% of all the phosphopeptides in IAV-infected and control samples were

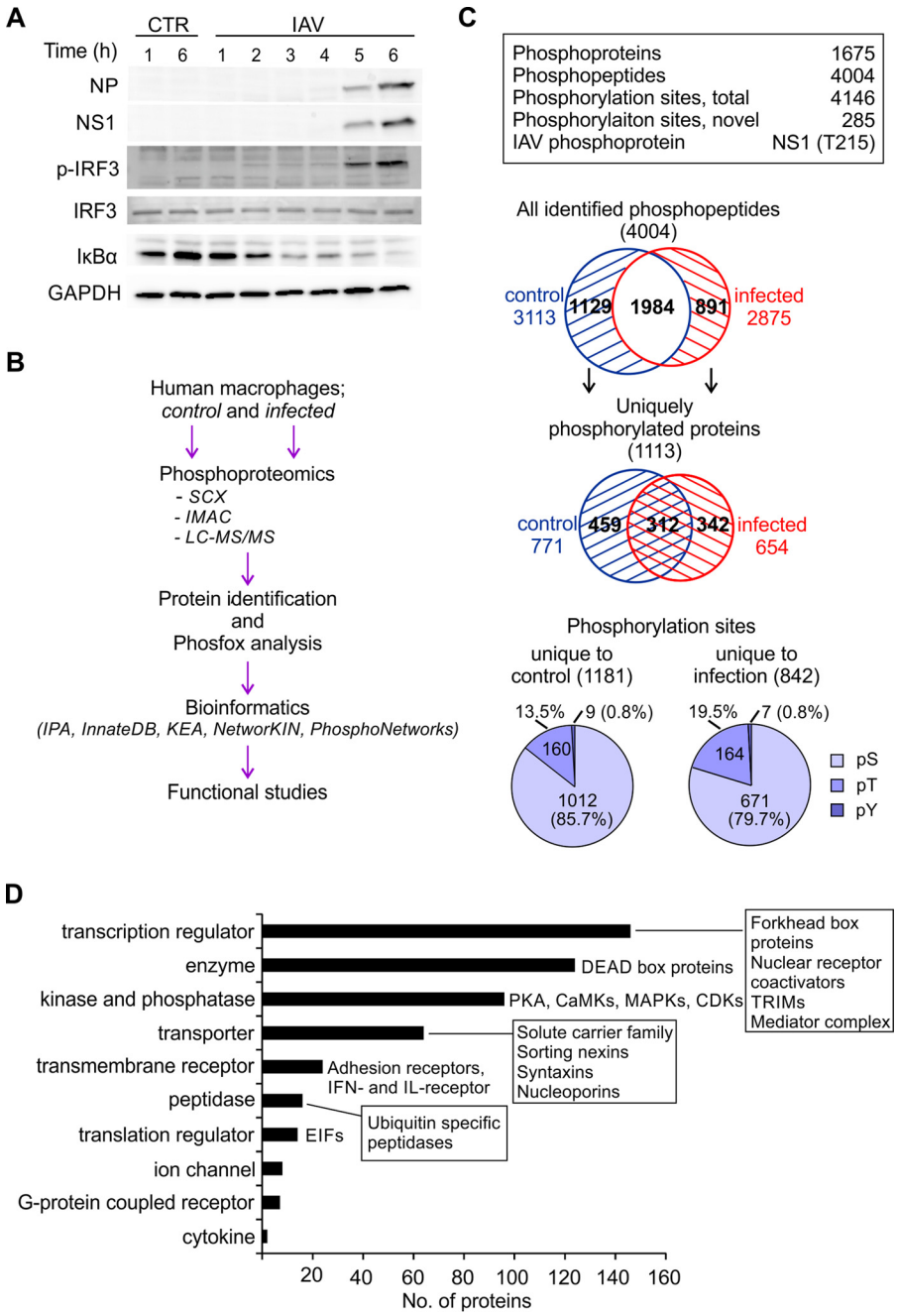

FIG. 1. **Phosphoproteome analysis of influenza A virus-infected primary human macrophages.** *A*, Macrophages were infected with influenza A virus for the times indicated. After this, total cell lysates were prepared and analyzed with Western blotting with anti-NP and anti-NS1, anti-phospho(Ser396)-IRF3, anti-IRF3 and anti-IκBα antibodies. Glyceraldehyde-3-phosphate dehydrogenase (GAPDH) detection was used to confirm equal sample loading. *B*, The workflow for the phosphoproteomics experiment. *C*, Phosphoprotein and -peptide identification results when pooling the identifications of both biological replicates. *D*, Classification of the uniquely phosphorylated proteins based on their molecular type. Ingenuity Pathway Analysis (IPA®) assigned a specific molecular type to 502 of the 1113 proteins identified as uniquely phosphorylated upon IAV infection.

identified in both replicates (supplemental Fig. S2 and Table S4), which is comparable to phosphoproteomic data sets that we published previously (11, 18). More detailed comparison of the phosphopeptide and -protein identification results revealed that altogether 507 human proteins showed reproducible qualitative changes in their phosphorylation profiles upon IAV infection (supplemental Fig. S2 and Table S4). From all of the identifications, 285 phosphorylation sites in 222 different proteins have not previously been reported in the PhosphoSitePlus (33), Phosida (34), or UniProt (http://www.uniprot.org/) databases,

and were therefore considered as "novel" phosphosites. The proportion of phosphoamino acids in the data set unique to control was ~86% pSer, 14% pThr, and 1% pTyr, whereas in the data set unique to infection the proportion of phosphorylated threonines was higher (approx. 80% pSer, 20% pThr, and 1% pTyr) (Fig 1C).

The LC-MS/MS analysis identified IAV proteins exclusively in the infected samples, and only one virus phosphopeptide, belonging to the NS1 protein, was identified with high confidence (Fig. 1*C*). This amino acid residue (Thr215) in the NS1 protein (Udorn IAV strain) was reported previously to be phosphorylated (35, 36), and it has been proposed that CDKs were the upstream kinases involved in NS1 phosphorylation (35). NS1 is the main viral protein that suppresses the innate anti-influenza immune responses in the host and it interferes with both IFN production and NLR family pyrin domain containing 3 (NLRP3) inflammasome activation (37–39). Furthermore, we recently reported that removing the NS1 C-terminal domain, which hosts Thr215, strongly reduces the capacity of IAV to antagonize antiviral responses in macrophages and in mice (40).

Transcription Regulators, Kinases and Phosphatases, and Transporters Are Differentially Phosphorylated During Influenza Virus Infection—To gain biological insight into the phosphoproteome data we performed in-depth bioinformatics characterization of the data sets. As the first step, the list of the 507 human proteins that were reproducible regulated in their phosphorylation status upon IAV infection was analyzed using the Ingenuity Pathway Analysis (IPA®) (supplemental Table S5). In addition, IPA analysis was done using the 1113 proteins identified as being regulated upon IAV in one of the biological replicates (supplemental Table S5). Classification based on known subcellular location revealed that most of the uniquely phosphorylated proteins had cytoplasmic or nuclear annotation, but several plasma membrane proteins were also identified. A specific annotated molecular type was found for 233 out of the 507 reproducibly identified phosphoproteins and for 502 out of the 1113 phosphoproteins identified in one of the biological experiments (approx. 45%). These phosphoproteins were mainly transcription regulators, kinases and phosphatases, other enzymes and transporters (Fig 1*D*). The transcription regulators included several distinct protein families such as forkhead box (FOX) proteins, nuclear receptor coactivators, tripartite motif family (TRIM) proteins and members of the mediator complex. This is in line with the previous studies that have linked FOX and TRIM proteins to host responses and control to viral infection (41–44). Our analysis also identified many enzymes involved in nucleic acid metabolism and energy production, such as DEAD box helicases. Kinases identified as uniquely phosphorylated during IAV infection included mitogen-activated protein kinases (MAPKs), as well as several members of CDK, Ca^{2+}/calmodulin-dependent kinase (CaMK) and cAMP-dependent protein kinase (PKA) families, which are known to be activated by various viruses (45–49). Transporters are involved in the movement of ions, small molecules, or macromolecules across biological membranes. During IAV infection, there is a dynamic transport of viral components from the plasma membrane to the nucleus and finally back to the plasma membrane (50–52). Our analysis showed changes in the phosphorylation of many transporters, such as solute carrier family members, sorting nexins, syntaxins and nucleoporins. Sorting nexins and syntaxins are involved in endocytosis and vesicle transport, whereas nucleoporins regulate the movement of macromolecules between the cell nucleus and the cytoplasm. Moreover, transmembrane receptors such as adhesion receptors and IFN- and IL-receptors, ubiquitin-specific peptidases and eukaryotic translation initiation factors (EIFs) were uniquely phosphorylated upon infection.

To determine which kinases are activated upon viral infection we used the Kinase Enrichment Analysis (KEA) (25). KEA is a standard tool for linking mammalian proteins with the kinases that phosphorylate them. To get a complete overview of activated kinases we used for this analysis all the uniquely phosphorylated proteins identified in the control and the infected samples (771 and 654 proteins, respectively). We identified ~20% of the phosphoproteins from the two phosphoproteome data sets as known kinase substrates (Table I and supplemental Table S6). In both samples, there was a significant overrepresentation of substrates for glycogen synthase kinase beta (GSK3B), MAPK14 (p38α), cyclin-dependent kinases CDK1 (CDC2), and CDK2. GSK3B has been shown before to be an important player in IAV entry (53). Recently, it was shown that GSK3B activation is needed for the expression of IRF3-regulated IFN-stimulated genes (54). The KEA analysis results included substrates of several members of the MAPK family (p38α, JNK2, ERK1, JNK1, ERK2, MAPKAPK5, MAPK10, MAPK11, and MAPK13) as highly enriched after infection. The MAPKs ERK1/2, p38, and JNK1/2 have been reported to be activated upon IAV infection (55–57). Especially p38 is considered the most important MAPK in the IAV infection-related immune response (58). Our results support these findings, demonstrating that many substrates of MAPKs are differently phosphorylated upon infection.

Other kinases whose known substrates were enriched in the phosphoproteins that were identified from IAV-infected macrophages included Serine/threonine-protein kinase PAK1 and Rho-associated coiled-coil containing protein kinase 2 (ROCK2). These two kinases are involved in the actin cytoskeleton regulation. PAK1, a target of Ras GTPases, is located upstream of interferon signaling molecules IKKε and TBK-1, which in turn phosphorylates IRF3 to induce IFN-β expression. ROCK2 is regulated by RhoA and RhoC, which belong to the Ras superfamily. ROCK2 plays a role in apoptosis, cell survival, and proliferation. In a siRNA screen where specific host membrane-trafficking genes were silenced, ROCK2 was identified as a cofactor in the hepatitis C virus replication (59). In our analysis, Ribosomal protein S6 kinase

TABLE I

Kinase Enrichment Analysis results. Kinase Enrichment Analysis of the uniquely phosphorylated proteins in the control (771 proteins) and the infected (654 proteins) samples. The results are listed according to significance of the IAV-infected sample, and the significance threshold for the kinases is set to $p < 0.05$

Kinase	Description	IAV infected *p* value	IAV infected Substrates in dataset	Control *p* value	Control Substrates in dataset	Substrates in KEA Database
GSK3B	Glycogen synthase kinase-3 beta	1.10E-10	49	1.59E-09	55	501
MAPK14	p38 alpha	4.18E-08	37	2.19E-08	44	377
CDC2	Cyclin-dependent kinase 1	1.12E-05	34	2.29E-08	47	421
CDK2	Cyclin-dependent kinase 2	1.39E-04	30	6.66E-07	42	398
MAPK9	JNK2	1.66E-04	15	8.68E-05	18	132
PRKCB1	Protein kinase C beta type	5.26E-04	21	0.00223	23	254
TRPM7	Transient receptor potential cation channel subfamily M member 7	8.23E-04	4	0.0824	2	9
PRKG1	cGMP-dependent protein kinase 1	9.42E-04	11	0.0149	10	93
MAPK10	JNK3	9.88E-04	12	0.00258	13	109
NEK9	Serine/threonine-protein kinase Nek9	0.00573	3	0.335	1	8
PAK1	Serine/threonine-protein kinase PAK 1	0.00661	8	0.130	6	72
PRKDC	DNA-dependent protein kinase catalytic subunit	0.00797	15	0.0145	17	200
SGK2	Serum/glucocorticoid-regulated kinase 2	0.00943	3	0.0176	3	10
MAPK3	ERK1	0.0115	13	0.176	11	170
MAPK8	JNK1	0.0137	16	0.0502	17	234
VRK1	Serine/threonine-protein kinase VRK1	0.0168	2	0.203	1	4
PBK	Lymphokine-activated killer T-cell-originated protein kinase	0.0171	3	0.140	2	13
SGK3	Serum/glucocorticoid-regulated kinase 3	0.0202	3	0.0367	3	14
MAPK1	ERK2	0.0234	15	0.120	15	229
DYRK1A	Dual specificity tyrosine-phosphorylation-regulated kinase 1A	0.0237	3	0.516	1	15
MAPKAPK5	MAP kinase-activated protein kinase 5	0.0274	3	0.188	2	16
ROCK2	Rho-associated protein kinase 2	0.0274	3	-0.00403	0	16
LATS1	Serine/threonine-protein kinase LATS1	0.0300	2	0.00588	3	6
RPS6KA5	Ribosomal protein S6 kinase alpha-5	0.0301	4	0.756	1	30
MAPK11	p38 beta	0.0314	3	0.558	1	17
MAPK13	Mitogen-activated protein kinase 13	0.0314	3	0.204	2	17
AKT1	RAC-alpha serine/threonine-protein kinase	0.0318	12	0.074	13	176

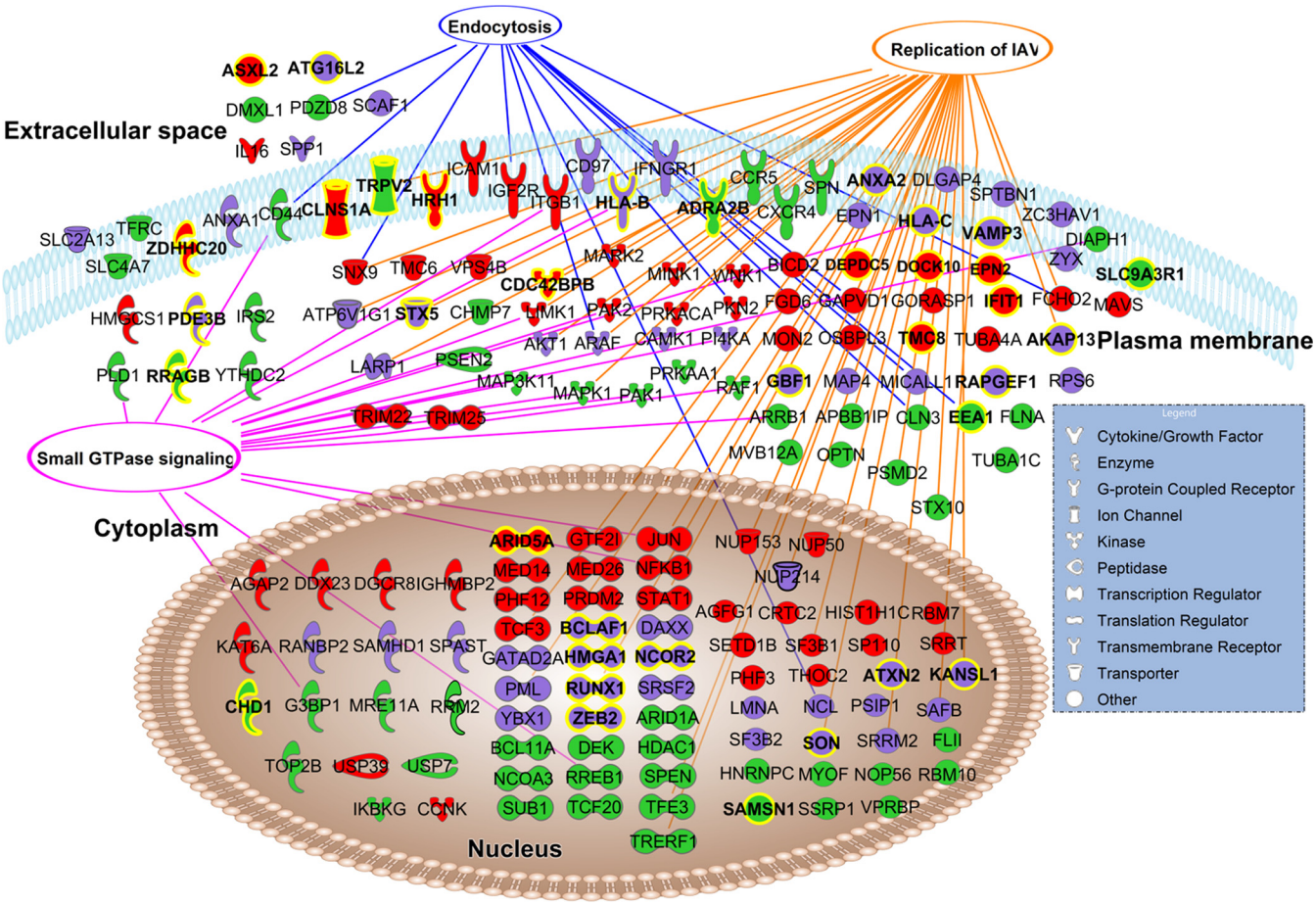

FIG. 2. **The phosphorylation profiles change upon influenza A virus infection for host proteins known to be involved in different stages of viral infection.** In total 180 proteins of the 1113 uniquely phosphorylated proteins were directly associated with the biological function "viral infection" according to IPA®, and 177 of these had annotated subcellular locations. These 177 proteins are shown and their molecular type is indicated by specific shapes. The purple nodes are proteins, which have unique phosphorylation sites in both uninfected (control) and infected conditions. The red nodes are proteins, which have unique phosphorylation sites only after infection. The green nodes are proteins that have unique phosphorylation sites only in the control sample. Proteins associated with small GTPase signaling (connected with magenta colored edges), replication of influenza A virus (connected with orange colored edges), and endocytosis (connected with blue colored edges) are highlighted with edges connected to the respective biological function. Phosphoproteins with novel phosphorylation sites are highlighted in bold text coding and yellow colored outlining.

alpha-5 (RPS6KA5), also known as mitogen- and stress-related kinase 1 (MSK-1), was enriched in the infected sample compared with control. RPS6KA5 has been described to play a role in innate inflammatory response, for instance in responses to human respiratory syncytial virus infection (60). Taken together, our results indicate that kinases with documented roles in cytoskeleton regulation, viral infection and replication, cell survival, and interferon signaling are activated upon IAV infection in primary macrophages.

Influenza A Virus Infection Changes the Phosphorylation of Many Host Proteins and Signaling Pathways Related to Viral Infection—One of the top biological functions in the pathway analysis was "Infectious disease," and within this category, the most significant annotated function was "Viral infection" (supplemental Table S5). From the 507 reproducibly regulated proteins upon IAV infection 99 were directly linked to viral infection (supplemental Table S5). Of all the 1113 proteins regulated by IAV infection, 180 proteins were directly associated with viral infection (Fig. 2). All the phosphorylated proteins regulated by IAV infection were further analyzed with the InnateDB database (23), which was developed explicitly for systems biology research on the innate immune system (supplemental Table S7). The KEGG pathway-based analysis was very similar to the IPA® results, showing that endocytosis, mTOR signaling, spliceosome, and RNA transport, all of which are important in the IAV life cycle, are enriched in the infected macrophage samples.

Viruses use host signaling pathways for promoting their life cycle, and consistently, our analysis showed here that several host factors which appear to be important for the replication of IAV were uniquely phosphorylated during infection. For example, twelve of the virus infection-associated phospho-

proteins that we identified have previously been linked to endocytosis, an early step in the IAV cellular replication cycle (Fig. 2). These include FCH domain only 2 (FCHO2), which has been described to regulate the early steps of clathrin-mediated endocytosis of IAV, and its silencing inhibited the replication of A/WSN/33 (H1N1) influenza virus (61). Small GTPase signaling was also activated during infection: Cdc42, Rac1 and Rho canonical signaling pathways were top pathways and several proteins associated with IAV infection were linked to small GTPase signaling (Fig. 2 and supplemental Table S5). G-protein-coupled receptors on the surface of phagocytes such as macrophages sense microbial presence and indirectly activate Rac, Rho, and Cdc42. These proteins transduce intracellular signaling leading to the production of reactive oxygen species, which increases the antimicrobial potency of macrophages. Rho signaling pathway has been linked to IAV uptake and internalization, as RhoA is thought to influence the Ca^{2+} response in IAV infected cells (51). Thus, both the IPA® results and the InnateDB database REACTOME pathway results (supplemental Table S7), with "Signaling by Rho GTPases" as the top scored pathway, strongly suggest an important role for Rho family of GTPases in regulating IAV replication and/or antiviral response.

Ubiquitination through the Lys63 residue of ubiquitin is associated with signal transduction, and the cross-talk between phosphorylation and ubiquitination is an emerging topic in the regulation of many signaling pathways. Furthermore, ubiquitination and deubiquitination critically regulate virus infection-induced type I IFN production. Two interesting proteins that were specifically phosphorylated in response to IAV infection were TRIM22 and TRIM25, which are ubiquitin E3 ligases. TRIM22 has been shown to restrict the replication of a number of viruses including encephalomyocarditis, hepatitis B, and human immunodeficiency viruses (62). Interestingly, TRIM22 inhibits IAV infection by targeting the viral NP for degradation (42). TRIM25 has been shown to be essential for RIG-I mediated antiviral activity (63). It interacts with RIG-I and delivers the Lys63-linked ubiquitin moiety to the second CARD domain on the N terminus of RIG-I, resulting in its binding to MAVS and a marked increase in RIG-I downstream signaling and type I interferon induction. Influenza A virus NS1 was shown to specifically counteract this TRIM25-mediated RIG-I CARD ubiquitination (43). In addition to ubiquitin conjugating enzymes, IAV infection induced phosphorylation of several ubiquitin carboxyl terminal hydrolases, which reverse the function of ubiquitin conjugating enzymes by hydrolyzing ubiquitin adducts. Of these, ubiquitin carboxyl terminal hydrolases 15 and 25 are of special interest. These two proteins have been shown to negatively regulate virus-induced type I IFN response (64, 65). Our data shows that carboxyl terminal hydrolases 15 and 25 are phosphorylated on Ser225 and Thr149, respectively, during IAV infection. Taken together, our data show that both ubiquitination and deubiquitination events are regulated by protein phosphorylation during IAV infection of human macrophages.

Mitochondria act as critical platforms for the assembly of signaling complexes that operate in innate immunity (66). It was recently shown that MAVS is phosphorylated in response to stimulation on two different C-terminal serine clusters, including Ser426/Ser430/Ser433 and Ser442/Ser444/Ser445/Ser446 residues (67). Of these, Ser442 phosphorylation was essential for MAVS interaction with IRF3, for IRF3 activation and type I IFN production. Our data shows that MAVS is phosphorylated on serine residues Ser165 and Ser222 in response to IAV infection. The Ser165 amino acid residue is part of a target sequence motif (pS/pTXR/K) of protein kinases PKA and PKC. The Ser222 amino acid residue, on the other hand, is situated in kinase substrate motifs of ERK1, ERK2, CDK5, GSK3, G protein coupled receptor kinase, and casein kinase I. Future studies are needed to elucidate the role of these phosphorylations in MAVS-induced innate immune response.

Cyclin-dependent Kinases are Activated Upon IAV Infection and Their Specific Inhibitors Rescue Primary Macrophages From Virus-induced Cell Death and Suppress IAV Replication—Next, the NetworKIN algorithm in KinomeXplorer (24) was used for predicting kinases associated with the unique phosphorylation sites. Of the identified 842 phosphosites unique to infection and 1181 unique to control (Fig 1*C*), kinases were predicted for 240 and 372 phosphosites, respectively (supplemental Table S8). Approximately 10% of the unique phosphorylation sites were predicted to be phosphorylated by cyclin-dependent kinases (see the separate sheet "CDK_sites" in supplemental Table S8 for details). Proteins which were differently phosphorylated upon IAV infection and identified by KEA or NetworKIN as substrates of CDK1 or CDK2 are shown in Fig 3*A*. In total 122 phosphoproteins were identified as CDK1 or/and CDK2 substrates; 34 were common for both samples, 55 were unique to the control and 33 unique to the IAV sample. The reproducibly identified phosphoproteins as CDK 1 and/or CDK2 substrates are shown in supplemental Table S9. In particular, several CDK1/2 substrates with unique phosphorylation sites identified after IAV infection were linked to virus host interaction. These included proteins known to be involved in transcriptional regulation, mRNA processing, clathrin-mediated endocytosis, and apoptosis. Of these serine/arginine-rich (SR) protein SRRM2 which is involved in messenger RNA splicing is especially interesting. It has been previously shown that SRRM2 is phosphorylated in HIV-1 infection specific manner. It was shown that HIV-1 modulates host cell alternative splicing machinery through SRRM2 during virus entry in order to facilitate virus replication and release (7). Our findings suggest a similar role for SRRM2 during IAV infection. Utilizing the PhosphoNetworks database (68), we further identified substrates for CDK7 and CDK9 in our phosphoproteome analysis (Fig 3*A*). All these analyses suggest that several CDKs are activated upon IAV infection.

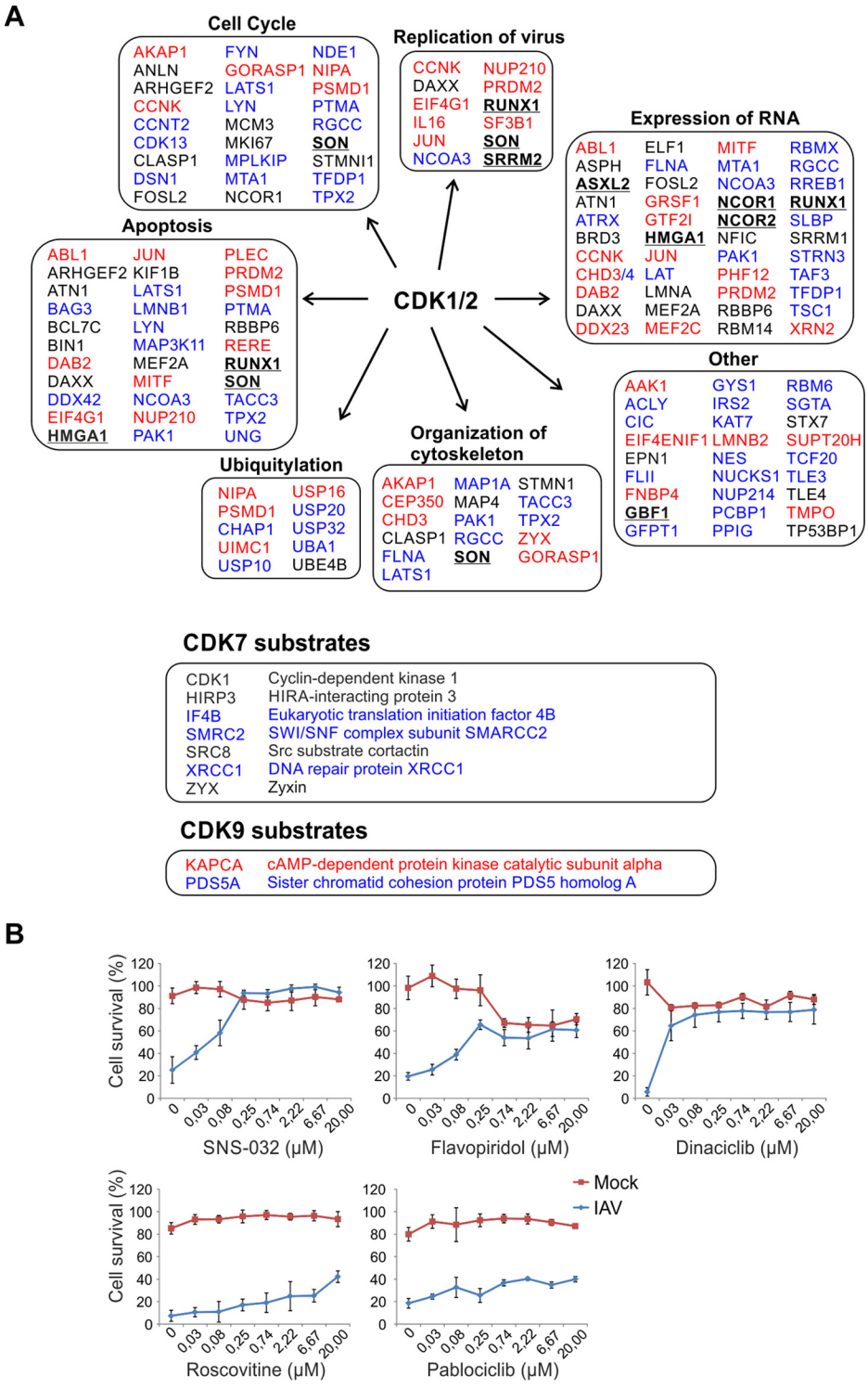

FIG. 3. **Cyclin-dependent kinases are activated upon influenza A virus infection, and their specific inhibitors rescue primary macrophages from virus-induced cell death.** *A*, The uniquely phosphorylated substrate proteins of CDK1, CDK2, CDK7, and CDK9 are shown with their gene names. The substrates for CDK1 and CDK2 are classified according to their biological process (note that one protein can belong to more than one class). Black colored coded proteins have unique phosphorylations in control and IAV samples, red colored coded proteins have unique phosphorylations only after IAV infection, and blue colored proteins have unique phosphorylations only in the untreated, control sample. The bold text coded proteins were identified to have novel phosphosites. *B*, Mock- or influenza A virus (MOI 3) infected primary macrophages were treated with increasing concentrations of various CDK inhibitors (SNS-032, flavopiridol, dinaciclib, roscovitine, and pablociclib). Cell viability was measured with the CTG assay at 24 h post-infection.

Interestingly, also a previous study had identified that CDK-related signaling events were overrepresented in the virus infection-associated phosphoproteome and that CDKs facilitate lytic gammaherpesvirus replication (8).

In addition to a large number of substrates for different CDKs we identified phosphopeptides from CDK11, CDK12, CDK13 in the phosphoproteomics data, suggesting that these could play a role in the IAV life cycle, in particular in primary macrophages, which do not undergo cell division. A proviral function has been attributed to CDK13 in lung epithelial cells (69), and a previously published siRNA screen also concluded that CDK13 is vital for IAV replication (70).

Cyclin-dependent kinases regulate several cellular processes, including the cell cycle, transcription, RNA processing, and cell survival. To study the role of CDKs in IAV-induced cell death and virus replication we used small molecule (molecular mass $<$ 900 Da) kinase inhibitors of CDKs (CDKIs). Pharmacological CDKIs have been originally developed to inhibit CDK signaling in Alzheimer's and Parkinson's disease, ischemia, and cancer. More recently, it was shown that CDKIs have antiviral activity against clinically important viruses including hepatitis C virus (71), human cytomegalovirus (72–74), human immunodeficiency virus type-1 (75–77), Epstein-Barr virus (78), and herpes simplex virus type 1 and 2 (79). These small molecule inhibitors have high specificity, good pharmacological properties and little side-effects (80, 81). Furthermore, safety data from numerous clinical trials are available for these drugs. First, we tested the effects of SNS-032, flavopiridol, dinaciclib, roscovitine, and pablociclib on the viability of noninfected (mock) and IAV-infected macrophages (MOI 3, Fig 3*B*). SNS-032, flavopiridol, and dinaciclib rescued macrophages from virus-mediated death at noncytotoxic concentrations at 24 h post-infection, whereas roscovitine and pablociclib did not have similar potency at the selected range of concentrations. Importantly, the protective effect of SNS-032 was lost when the drug was added to the IAV-infected cells later than 3 h post-infection (supplemental Fig. S3*A*). We propagated the viruses at MOI 0.01 in macrophages pre-treated at different compound concentrations and calculated the half maximum effective concentrations (EC_{50}), half maximum cytotoxic concentrations (CC_{50}), and selectivity indexes (SI) for both SNS-032 and flavopiridol (supplemental Fig. S3*B*). With an EC_{50} of 40 nM and a SI $>$ 500, the SNS-032 proved to be a potent small molecule inhibitor of IAV-associated cellular cytotoxicity in primary human macrophages.

Based on these experiments, we decided to characterize the effects of SNS-032 and flavopiridol (EC_{50} = 200 nM and SI $>$ 100) on IAV-infected human macrophages in more detail. RT-qPCR analysis showed that both SNS-032 (0.3 μM) and flavopiridol (0.3 μM) inhibit expression of viral *M2* and *NP* mRNAs in macrophages that were infected with IAV for 6 h (Fig 4*A*). In line with this result, these CDKIs also blocked the expression of viral NS1 and NP proteins in macrophages that had been infected with IAV for 18 h (Fig 4*B*). Thus, it is highly likely that these CDKIs inhibit IAV replication.

Selected Cyclin-dependent Kinase Inhibitors Suppress Antiviral and Chemokine Response in IAV-infected Human Macrophages—Human macrophages respond to IAV infection by producing antiviral cytokines, including type I and III IFNs and chemokines that can attract other immune cells to the site of infection. To study the effect of CDKIs on IAV-induced antiviral cytokine and chemokine response, macrophages were infected with IAV for 6 h in the presence and absence of CDKIs. After this, total cellular RNA was isolated, cDNA was prepared and the expression of IFNs and chemokines was analyzed by RT-PCR. The inhibitors had modest, but significant, effect on IAV infection-induced IFN-β mRNA levels (Fig 4*C*). In contrast, both flavopiridol and SNS-032 treatment completely abolished IAV infection-induced expression of *IL-29 (IFN-λ1)*, *CXCL10*, and *CXCL11* genes (Fig 4*C*). Flavopiridol or SNS-032 administration did not affect *GAPDH* or *18S* ribosomal RNA expression, indicating that these inhibitors do not interfere with the general cellular transcription (supplemental Fig. S4).

Next, we analyzed with the cytokine array proteome profiler the production of pro-inflammatory cytokines and chemokines from cell culture supernatants of IAV-infected human macrophages in the presence or absence of CDKIs. The secretion of chemokines CCL2, CCL3, CCL4, RANTES (CCL5), and CXCL10 was completely abolished by flavopiridol or SNS-032 in IAV-infected human macrophages (S5A Fig). Similarly, the secretion of cytokines IL-6 and IL-16 as well as complement component C5/C5a was totally inhibited by CDKI-treatment. Interestingly, the CDKIs only partially inhibited TNF secretion in response to IAV infection. This result was confirmed with ELISA, which showed that the decrease in TNF secretion attained statistical significance after flavopiridol, but not after SNS-032 administration (supplemental Fig. S5*B*).

IRF3 and NF-κB signaling pathways are involved in the activation of antiviral and pro-inflammatory response during viral infections, and we studied the effect of SNS-032 on these signaling pathways during IAV infection. Human macrophages were infected with IAV for 6 h in the absence and presence of SNS-032 after which cell lysates were prepared and Western blot analysis was performed with anti-phospho IRF3 and anti-IκBα antibodies (Fig 4*D*). SNS-032-treatment clearly but not completely inhibited the IAV-induced phosphorylation and activation of IRF3. The *IFN-β* promoter has been shown to have a very high affinity for activated IRF3 compared with other antiviral genes (82). Therefore, the expression of IFN-β can be induced by IRF3 that is only modestly phosphorylated which was seen in SNS-032 treated and IAV-infected macrophages (Figs. 4*C* and 4*D*). Interestingly, SNS-032 alone induced degradation of IκBα demonstrating activation of NF-κB. Furthermore, IκBα was almost completely lost in SNS-032-treated and IAV-infected human

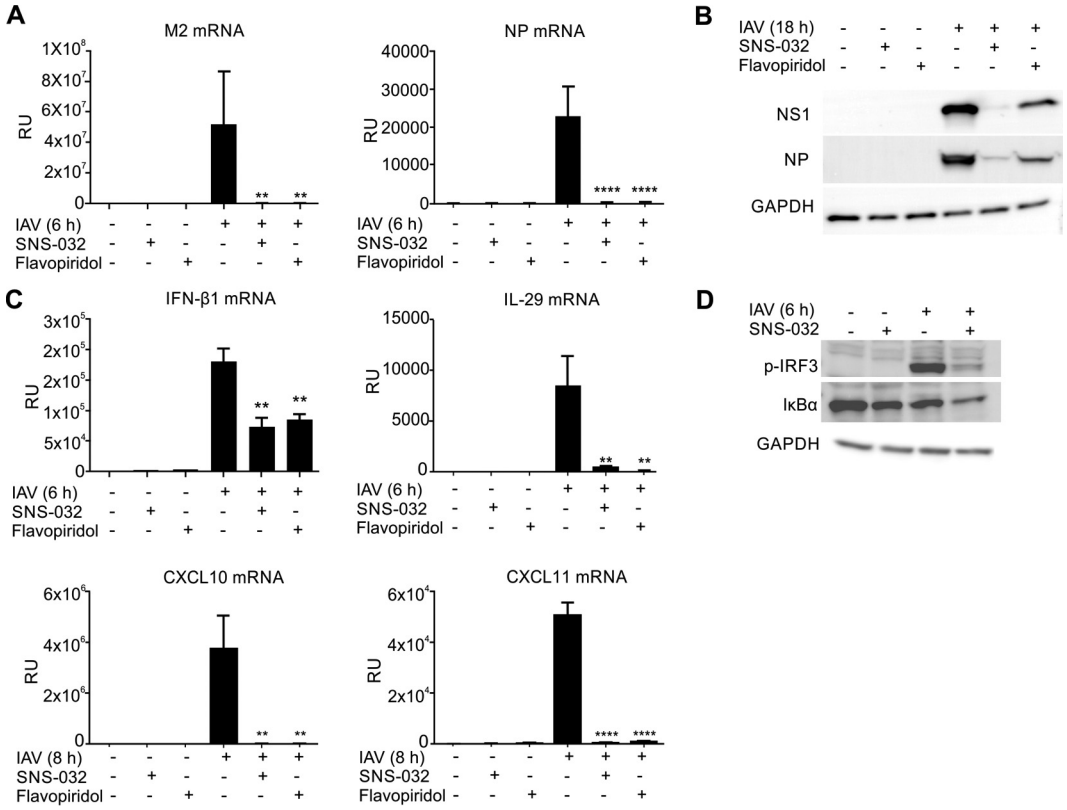

FIG. 4. **The effect of cyclin-dependent kinase inhibitors on virus replication and antiviral and chemokine response in influenza A virus-infected human macrophages.** *A*, Primary human macrophages differentiated from three donors were pretreated with CDK inhibitors SNS-032 (0.3 μM) or flavopiridol (0.3 μM) for 1 h after which they were left uninfected or infected with IAV for 6 h. After this, the cells from the separate donors were collected and pooled, and total cellular RNA was prepared. The mRNA expression of IAV *M2* and *NP* genes was analyzed with quantitative RT-PCR. Data is presented as mean and S.D. of $n = 3$ independent measurements. The results were compared with the infected and untreated sample. *B*, Primary human macrophages differentiated from three donors were pretreated with CDK inhibitors of SNS-032 (0.3 μM) or flavopiridol (0.3 μM) 1 h before infection. The protein abundances of influenza A virus NS1 and NP proteins 18 h post-infection were measured with Western blotting, using GAPDH as a loading control. *C*, Primary human macrophages differentiated from three donors were pretreated with CDK inhibitors of SNS-032 (0.3 μM) or flavopiridol (0.3 μM) 1 h before infection. The expression of *IFN-β*, *IL-29*, *CXCL10*, and *CXCL11* mRNAs in IAV infected macrophages was analyzed with quantitative RT-PCR. Data is presented as mean and S.D. of $n = 3$ independent measurements. The results were compared with the infected and untreated sample. *D*, Macrophages were pretreated with SNS-032 (0.3 μM) for 1 h after which they were left uninfected or infected with IAV for 6 h. After this, the cell lysates were prepared and analyzed with Western blotting with anti-phospho-IRF3 and anti-IκBα antibodies. Comparable data were obtained from two different experiments.

macrophages indicating robust activation of NF-κB under these conditions. In conclusion, these results show that SNS-032 differentially regulates IRF3 and NF-κB signaling pathways.

CDKIs Abrogate Apoptosis and Inflammasome Activation in IAV-infected Macrophages—IAV infection of human macrophages is associated with apoptosis of the infected cells (83). We therefore decided to study the effect of SNS-032 and flavopiridol on IAV-induced apoptosis. There are two main apoptotic pathways, the extrinsic pathway, regulated by activation of extracellular death receptors that functions through caspase 8, and the intrinsic pathway that functions through caspase 9 and is initiated by the disruption of the mitochondrial membrane potential. Both caspase 8 and 9 activate caspase 3 by proteolytic cleavage. Caspase 7 is also a downstream effector protease of the apoptotic pathway. The activity of caspases 3/7, 8, and 9 was measured with the Caspase-Glo assay in human macrophages that were infected with IAV in the presence and absence of SNS-032. IAV infection of human macrophages clearly enhanced caspase 3/7 activity at 18 h post-infection and this activation was completely inhibited by SNS-032 (Fig 5*A*). Similarly, the activity of caspase 9 was induced by IAV infection and decreased after SNS-032 or flavopiridol treatment. However, caspase 8 activity was comparable in mock and IAV-infected macrophages and SNS-032 or flavopiridol had no influence on the activity of caspase 8 in the macrophages. The inhibiting effect of CDKIs on IAV-induced caspase 3 activation was confirmed by Western blotting: both SNS-032 and flavopiridol inhibited the appearance of active 17/19 kDa fragment of caspase 3 induced by IAV infection (Fig 5*B*). In accordance with this result, both CDKIs abrogated the up-regulation of

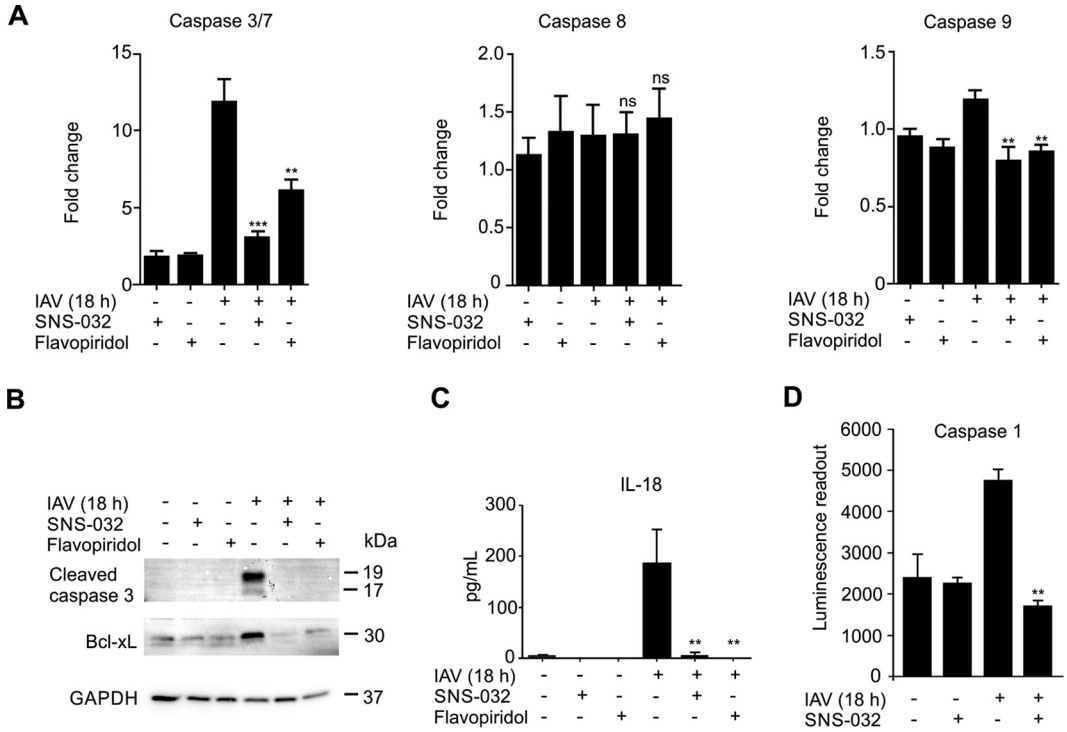

FIG. 5. **Cyclin-dependent kinase inhibitors block influenza A virus-induced apoptosis and inflammasome activation.** *A*, Macrophages were pretreated with SNS-032 (0.3 μM) or flavopiridol (0.3 μM) for 1 h after which they were left uninfected or infected with IAV for 18 h. Caspase 3/7, caspase 8, and caspase 9 activity was measured as described under Experimental Procedures. The changes in activity were calculated and compared with the mock/untreated sample (= 1). Data is presented as mean and S.D. of $n = 3$ biological replicates. The results were compared with the infected and untreated sample. *B*, Macrophages were pretreated with SNS-032 (0.3 μM) or flavopiridol (0.3 μM) for 1 h after which they were left uninfected or infected with IAV for 18 h. After this, total cell lysates were prepared and expression of cleaved caspase 3 (Asp175) and Bcl-xL expression was analyzed with Western blotting. *C*, Macrophages from three different donors were pretreated with SNS-032 (0.3 μM) or flavopiridol (0.3 μM) after which they were infected with IAV for 18 h. After this, the cell culture supernatants were collected and IL-18 secretion was analyzed with a Luminex assay. Data is presented as mean and S.D. of $n = 3$ independent measurements. The results were compared with the infected and untreated sample. *D*, The activity of caspase 1 was measured in 18 h infected or noninfected macrophages, nontreated or treated with SNS-032 at 0.3 μM at 18 h post-infected. Data is presented as mean and S.D. of $n = 3$ biological replicates. The results were compared with the infected and untreated sample.

Bcl-xL. Bcl-xL is an anti-apoptotic protein whose expression can be induced in response to IAV infection (84). Bcl-xL is a component of a cell signaling network that governs cell survival and cell death by interacting with pro-apoptotic proteins such as Bad and Bax (85). The expression of Bcl-xL is regulated by NF-κB and other transcription factors, *e.g.* CREB and STATs. JAKs and Src kinases phosphorylate and activate STAT3, which is known to induce the expression of Bcl-xL (86). It is possible that in the absence of IFNs and other cytokines in infected but SNS-032 treated cells, the JAK and Src signaling pathways are not activated and the expression of Bcl-xL is not induced.

IAV infection of human macrophages is associated with caspase 1 activation and the subsequent secretion of pro-inflammatory cytokines IL-18 and IL-1β (16). Caspase 1 is activated in a molecular platform called NLRP3 inflammasome, comprising the protein NLRP3, the adaptor apoptosis-associated speck-like protein (ASC) and pro-caspase 1. The NLRP3 inflammasome has been shown to be essential for the activation of host response during IAV infection (87, 88). To study the effect of CDKIs on NLRP3 inflammasome activation we infected human macrophages in the presence and absence of SNS-032 and flavopiridol and analyzed IL-18 secretion and caspase 1 activation. Our results show that these CDKIs completely block IAV-induced secretion of IL-18 (Fig 5*C*). The activity of caspase 1 was increased in human primary macrophages after 18 h of IAV infection and this activity was significantly decreased when cells were treated with SNS-032 before infection (Fig 5*D*). These data demonstrate that the CDKIs prevent NLRP3 inflammasome activation. It is likely that CDKIs, and especially SNS-032, block IAV life cycle before the NLRP3 inflammasome can be assembled and activated.

CDKIs Protect Against IAV Challenge in Mice—Finally, we decided to validate the protective potential of the observed antiviral effects of SNS-032 *in vivo* in a standard mouse model for influenza infection. As a challenge virus, we used A/Puerto Rico/8/34 (PR8) virus because this virus is very well adapted to mice meaning that it causes disease in *e.g.* BALB/c mice after inoculation with as little as 10 plaque forming units. In

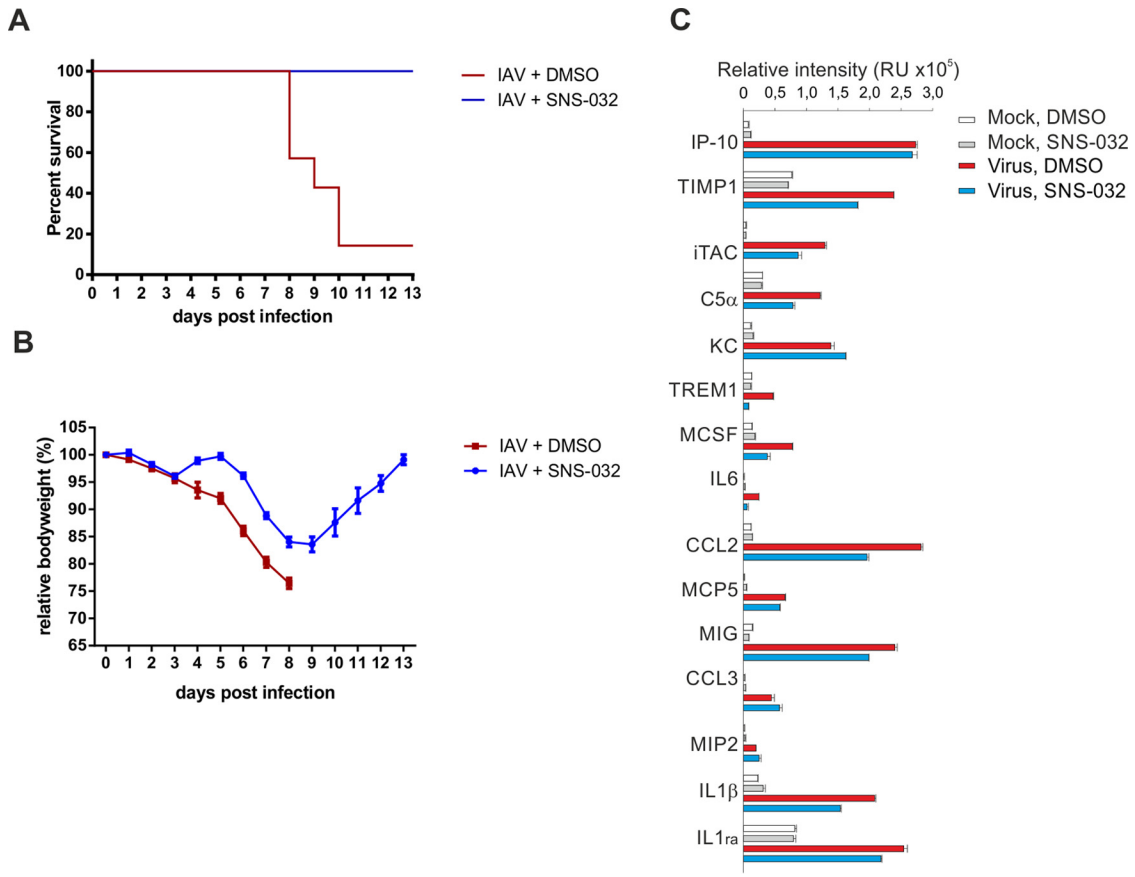

FIG. 6. **SNS-032 treatment rescues influenza A virus-infected mice.** Mortality and morbidity of SNS-032 treated and DMSO treated mice after lethal influenza infection. At day 0 the mice were infected with 0.5 LD_{50} of mouse-adapted PR8 or mock infected. Six mice per group were repeatedly treated intraperitoneally with SNS-032 at 1 day prior and 1, 3, 5, 7, and 9 days post infection. *A*, Kaplan-Meier survival curves of the infected mice show perfect protection gained by SNS-032 treatment (log-rank test, $p < 0.01$). *B*, Relative body weight curves for the two different groups of infected mice. SNS-032 treated mice lost significantly less body weight than the DMSO treated mice at days 4–7 (two-way ANOVA, Bonferroni's multiple comparison adjustment, $p < 0.0001$). At 9 days post infection more than half of the DMSO treated mice had died and hence from day 9 on, the body weight of the surviving DMSO treated mice was not included in the figure. *C*, Cytokine levels in mouse lung homogenates at day 5 were determined using mouse cytokine array panel A kit. Lung homogenates from four mice per group were combined before measuring the relative intensity of the luminescence for the different cytokines. Representative results from two experiments are shown.

addition, this virus productively infects murine macrophages (89). We focused on SNS-032 because it showed better antiviral activity *in vitro* compared with other CDKIs. In a first experiment female BALB/c mice (6 mice/group) were treated with SNS-032 (15 mg/kg in 5% DMSO) or vehicle (5% DMSO) administered intraperitoneally every other day, starting on day 1 before and until day 9 after infection. For infection we used 0.5 LD_{50} (corresponding to 20 plaque forming units per mouse) of mouse adapted PR8 strain. Kaplan-Meier survival analysis showed that 100% of the SNS-032-treated animals PR8 infection, whereas 83% DMSO-treated died from the influenza infection (or had to be euthanized because of excessive weight loss) (Fig 6*A* and 6*B*). Accordingly, SNS-032-treated animals lost significantly less body weight as compared with DMSO-treated animals.

We also observed an imbalance in the cytokine production in SNS-032-treated PR8-infected mice in comparison with vehicle-treated PR8-infected animals (Fig 6*C*). In particular, the levels of TIMP1, iTAC, C5a, TREM1, M-CSF, IL6, CCL-2, MIG, IL-1b, and IL-1ra were decreased by SNS-032 treatment in the infected animals. In aggregate, the tempered cytokine profile probably delayed the onset of severe disease in the mice up to a point where the adaptive immune response against the virus was capable of controlling and eliminating the infection.

Concluding Remarks—Like all other viruses, influenza A viruses rely on host factors for their life cycle; they manipulate and hijack cellular proteins for promoting their uptake, replication, and egress. Knowing the molecular mechanisms behind these events, for instance, how the viruses impact host cellular processes through protein phosphorylation, is important for understanding how viral diseases progress and for developing new antiviral treatments. Here, we took a mass spectrometry-based phosphoproteomics approach com-

bined with bioinformatics and functional studies to elucidate the host-response to influenza A virus infection in primary human macrophages. The focus was on the early phase of infection, corresponding to the time frame in which innate immune responses are typically initiated. Our data shows that there are phosphorylation changes in the host proteins involved in all critical stages of viral replication including entry, gene regulation and egress. Our results also highlight the importance of using primary cells in proteome-level studies to obtain novel and biologically most meaningful data for further functional studies. An important finding of our work is the remarkably altered phosphorylation status of several cyclin-dependent kinases and their substrates following IAV infection. Functional studies based on well-characterized small molecule CDK inhibitors showed that the CDK activity is required for efficient viral replication and for the activation of host response *in vitro*. Further, *in vivo* experiments showed that SNS-032, one of the selected CDKIs, could rescue IAV-infected mice.

In conclusion, we provide the first comprehensive phosphoproteome characterization of IAV infection in primary human macrophages, and provide extensive evidence that specific CDK inhibitors could be excellent candidates to treat severe influenza virus infections.

Acknowledgments—We thank Professor Ilkka Julkunen for the influenza A/Udorn/307/1972 virus and the anti-influenza A virus antibodies, Dr Ville Veckman for the influenza A virus primers, and Sari Tillander for her assistance with the Luminex analyses. Jens Desloovere is acknowledged for the assistance with the compound efficacy testing. We also thank Laura Turunen for her excellent assistance with drugging compounds and Liesbeth Vande Ginste for excellent technical support with mice experiments. Arttu Heinonen and Pekka Haapaniemi are acknowledged for the instrument support at the Turku Proteomics Facility and personnel at the High-Throughput Biomedicine Unit (FIMM Technology Centre, Helsinki, Finland) are acknowledged for their expert technical support. Research infrastructure support was provided by Biocenter Finland.

* This work was supported by grants from the Academy of Finland (grants 135 628, 140 950, 272 931, 255 842, 272437, 269862, 279163, 292611, and 295504), Integrative Life Science Doctoral Program (SS), Institute of Biotechnology (SS), and Orion Research Foundation (SS).

S This article contains supplemental material.

|| To whom correspondence should be addressed: Institute of Clinical Medicine, University of Oslo, Postboks 4950 Nydalen, 0424 Oslo, Norway. Tel.: +47 230 73017; E-mail: tuula.nyman@medisin.uio.no.

[a] Current address: Faculty of Pharmacy, Meijo University, Nagoya 468-8503, Japan.

[b] Current address: Van't Hoff Institute of Molecular Sciences, 1090 GS Amsterdam, the Netherlands.

[c] These authors contributed equally to this work.

REFERENCES

1. Flannery, B., Clippard, J., Zimmerman, R. K., Nowalk, M. P., Jackson, M. L., Jackson, L. A., Monto, A. S., Petrie, J. G., McLean, H. Q., Belongia, E. A., Gaglani, M., Berman, L., Foust, A., Sessions, W., Thaker, S. N., Spencer, S., Fry, A. M., and Centers for Disease Control and Prevention.(2015) Early estimates of seasonal influenza vaccine effectiveness - united states, january 2015. MMWR Morb. Mortal. Wkly. Rep. **64,** 10–15
2. Spanakis, N., Pitiriga, V., Gennimata, V., and Tsakris, A. (2014) A review of neuraminidase inhibitor susceptibility in influenza strains. Expert Rev. *Anti Infect. Ther.* **12,** 1325–1336
3. Hurt, A. C. (2014) The epidemiology and spread of drug resistant human influenza viruses. *Curr. Opin. Virol.* **8C,** 22–29
4. Greco, T. M., Diner, B. A., and Cristea, I. M. (2014) The impact of mass Spectrometry–Based proteomics on fundamental discoveries in virology. *Ann. Rev. Virol.* **1,** 581–604
5. Meissner, F., and Mann, M. (2014) Quantitative shotgun proteomics: Considerations for a high-quality workflow in immunology. *Nat. Immunol.* **15,** 112–117
6. Liu, Z., Wang, Y., and Xue, Y. (2013) Phosphoproteomics-based network medicine. *FEBS J.* **280,** 5696–5704
7. Wojcechowskyj, J. A., Didigu, C. A., Lee, J. Y., Parrish, N. F., Sinha, R., Hahn, B. H., Bushman, F. D., Jensen, S. T., Seeholzer, S. H., and Doms, R. W. (2013) Quantitative phosphoproteomics reveals extensive cellular reprogramming during HIV-1 entry. *Cell. Host Microbe* **13,** 613–623
8. Stahl, J. A., Chavan, S. S., Sifford, J. M., MacLeod, V., Voth, D. E., Edmondson, R. D., and Forrest, J. C. (2013) Phosphoproteomic analyses reveal signaling pathways that facilitate lytic gammaherpesvirus replication. *PLoS Pathog*. **9**, e1003583
9. Luo, R., Fang, L., Jin, H., Wang, D., An, K., Xu, N., Chen, H., and Xiao, S. (2014) Label-free quantitative phosphoproteomic analysis reveals differentially regulated proteins and pathway in PRRSV-infected pulmonary alveolar macrophages. *J. Proteome Res.* **13,** 1270–1280
10. Popova, T. G., Turell, M. J., Espina, V., Kehn-Hall, K., Kidd, J., Narayanan, A., Liotta, L., Petricoin EF3rd, Kashanchi, F., Bailey, C., and Popov, S. G. (2010) Reverse-phase phosphoproteome analysis of signaling pathways induced by rift valley fever virus in human small airway epithelial cells. *PLoS ONE* **5,** e13805
11. Ohman, T., Soderholm, S., Paidikondala, M., Lietzen, N., Matikainen, S., and Nyman, T. A. (2015) Phosphoproteome characterization reveals that sendai virus infection activates mTOR signaling in human epithelial cells. *Proteomics* **15,** 2087–2097
12. Oberstein, A., Perlman, D. H., Shenk, T., and Terry, L. J. (2015) Human cytomegalovirus pUL97 kinase induces global changes in the infected cell phosphoproteome. *Proteomics* **15,** 2006–2022
13. Medzhitov, R. (2008) Origin and physiological roles of inflammation. *Nature* **454,** 428–435
14. Hashimoto, Y., Moki, T., Takizawa, T., Shiratsuchi, A., and Nakanishi, Y. (2007) Evidence for phagocytosis of influenza virus-infected, apoptotic cells by neutrophils and macrophages in mice. *J. Immunol.* **178,** 2448–2457
15. Lietzen, N., Ohman, T., Rintahaka, J., Julkunen, I., Aittokallio, T., Matikainen, S., and Nyman, T. A. (2011) Quantitative subcellular proteome and secretome profiling of influenza A virus-infected human primary macrophages. *PLoS Pathog.* **7,** e1001340
16. Pirhonen, J., Sareneva, T., Kurimoto, M., Julkunen, I., and Matikainen, S. (1999) Virus infection activates IL-1 beta and IL-18 production in human macrophages by a caspase-1-dependent pathway. *J. Immunol.* **162,** 7322–7329
17. Francis, T., and Magill, T. P. (1935) Immunological studies with the virus of influenza. *J. Exp. Med.* **62,** 505–516
18. Ohman, T., Soderholm, S., Hintsanen, P., Valimaki, E., Lietzen, N., MacKintosh, C., Aittokallio, T., Matikainen, S., and Nyman, T. A. (2014) Phosphoproteomics combined with quantitative 14–3-3-affinity capture identifies SIRT1 and RAI as novel regulators of cytosolic dsRNA recognition pathway. *Mol. Cell. Proteomics* **13,** 2604–2617
19. Kauko, O., Laajala, T. D., Jumppanen, M., Hintsanen, P., Suni, V., Haapaniemi, P., Corthals, G., Aittokallio, T., Westermarck, J., and Imanishi, S. Y. (2015) Label-free quantitative phosphoproteomics with novel pairwise abundance normalization reveals synergistic RAS and CIP2A signaling. *Sci. Rep.* **5,** 13099
20. Vizcaino, J. A., Deutsch, E. W., Wang, R., Csordas, A., Reisinger, F., Rios, D., Dianes, J. A., Sun, Z., Farrah, T., Bandeira, N., Binz, P. A., Xenarios, I., Eisenacher, M., Mayer, G., Gatto, L., Campos, A., Chalkley, R. J., Kraus, H. J., Albar, J. P., Martinez-Bartolome, S., Apweiler, R., Omenn, G. S., Martens, L., Jones, A. R., and Hermjakob, H. (2014) Proteome-

Xchange provides globally coordinated proteomics data submission and dissemination. *Nat. Biotechnol.* **32,** 223–226
21. Taus, T., Kocher, T., Pichler, P., Paschke, C., Schmidt, A., Henrich, C., and Mechtler, K. (2011) Universal and confident phosphorylation site localization using phosphoRS. *J. Proteome Res.* **10,** 5354–5362
22. Soderholm, S., Hintsanen, P., Ohman, T., Aittokallio, T., and Nyman, T. A. (2014) PhosFox: A bioinformatics tool for peptide-level processing of LC-MS/MS-based phosphoproteomic data. *Proteome Sci.* **12**, 36–5956-12–36. eCollection 2014
23. Breuer, K., Foroushani, A. K., Laird, M. R., Chen, C., Sribnaia, A., Lo, R., Winsor, G. L., Hancock, R. E., Brinkman, F. S., and Lynn, D. J. (2013) InnateDB: Systems biology of innate immunity and beyond–recent updates and continuing curation. *Nucleic Acids Res.* **41,** D1228–D33
24. Horn, H., Schoof, E. M., Kim, J., Robin, X., Miller, M. L., Diella, F., Palma, A., Cesareni, G., Jensen, L. J., and Linding, R. (2014) KinomeXplorer: An integrated platform for kinome biology studies. *Nat. Methods* **11,** 603–604
25. Lachmann, A., and Ma'ayan, A. (2009) KEA: Kinase enrichment analysis. *Bioinformatics* **25,** 684–686
26. Denisova, O. V., Soderholm, S., Virtanen, S., Von Schantz, C., Bychkov, D., Vashchinkina, E., Desloovere, J., Tynell, J., Ikonen, N., Theisen, L. L., Nyman, T. A., Matikainen, S., Kallioniemi, O., Julkunen, I., Muller, C. P., Saelens, X., Verkhusha, V. V., and Kainov, D. E. (2014) Akt inhibitor MK2206 prevents influenza pH1N1 virus infection in vitro. *Antimicrob. Agents Chemother.* **58,** 3689–3696
27. Osterlund, P., Veckman, V., Siren, J., Klucher, K. M., Hiscott, J., Matikainen, S., and Julkunen, I. (2005) Gene expression and antiviral activity of alpha/beta interferons and interleukin-29 in virus-infected human myeloid dendritic cells. *J. Virol.* **79,** 9608–9617
28. Ohman, T., Lietzen, N., Valimaki, E., Melchjorsen, J., Matikainen, S., and Nyman, T. A. (2010) Cytosolic RNA recognition pathway activates 14–3-3 protein mediated signaling and caspase-dependent disruption of cytokeratin network in human keratinocytes. *J. Proteome Res.* **9,** 1549–1564
29. Sato, M., Suemori, H., Hata, N., Asagiri, M., Ogasawara, K., Nakao, K., Nakaya, T., Katsuki, M., Noguchi, S., Tanaka, N., and Taniguchi, T. (2000) Distinct and essential roles of transcription factors IRF-3 and IRF-7 in response to viruses for IFN-alpha/beta gene induction. *Immunity* **13,** 539–548
30. Weber, A., Wasiliew, P., and Kracht, M. (2010) Interleukin-1 (IL-1) pathway. *Sci. Signal.* **3**, cm1
31. Heylbroeck, C., Balachandran, S., Servant, M. J., DeLuca, C., Barber, G. N., Lin, R., and Hiscott, J. (2000) The IRF-3 transcription factor mediates sendai virus-induced apoptosis. *J. Virol.* **74,** 3781–3792
32. Chattopadhyay, S., and Sen, G. C. (2010) IRF-3 and bax: A deadly affair. *Cell. Cycle* **9,** 2479–2480
33. Hornbeck, P. V., Kornhauser, J. M., Tkachev, S., Zhang, B., Skrzypek, E., Murray, B., Latham, V., and Sullivan, M. (2012) PhosphoSitePlus: A comprehensive resource for investigating the structure and function of experimentally determined post-translational modifications in man and mouse. *Nucleic Acids Res.* **40,** D261–D70
34. Gnad, F., Gunawardena, J., and Mann, M. (2011) PHOSIDA 2011: The posttranslational modification database. *Nucleic Acids Res.* **39,** D253–D60
35. Hale, B. G., Knebel, A., Botting, C. H., Galloway, C. S., Precious, B. L., Jackson, D., Elliott, R. M., and Randall, R. E. (2009) CDK/ERK-mediated phosphorylation of the human influenza A virus NS1 protein at threonine-215. *Virology* **383,** 6–11
36. Hsiang, T. Y., Zhou, L., and Krug, R. M. (2012) Roles of the phosphorylation of specific serines and threonines in the NS1 protein of human influenza A viruses. *J. Virol.* **86,** 10370–10376
37. Hale, B. G., Randall, R. E., Ortin, J., and Jackson, D. (2008) The multifunctional NS1 protein of influenza A viruses. *J. Gen. Virol.* **89,** 2359–2376
38. Stasakova, J., Ferko, B., Kittel, C., Sereinig, S., Romanova, J., Katinger, H., and Egorov, A. (2005) Influenza A mutant viruses with altered NS1 protein function provoke caspase-1 activation in primary human macrophages, resulting in fast apoptosis and release of high levels of interleukins 1beta and 18. *J. Gen. Virol.* **86,** 185–195
39. Cheong, W. C., Kang, H. R., Yoon, H., Kang, S. J., Ting, J. P., and Song, M. J. (2015) Influenza A virus NS1 protein inhibits the NLRP3 inflammasome. *PLoS ONE* **10**, e0126456
40. Anastasina, M., Schepens, B., Soderholm, S., Nyman, T. A., Matikainen, S., Saksela, K., Saelens, X., and Kainov, D. E. (2015) The C-terminus of NS1 protein of influenza A/WSN/1933(H1N1) virus modulates antiviral responses in infected human macrophages and mice. *J. Gen. Virol.* **96,** 2086–2091
41. Okumura, N., Ikeda, M., Satoh, S., Dansako, H., Sugiyama, M., Mizokami, M., and Kato, N. (2015) Negative regulation of hepatitis B virus replication by forkhead box protein A in human hepatoma cells. *FEBS Lett.* **589,** 1112–1118
42. Di Pietro, A., Kajaste-Rudnitski, A., Oteiza, A., Nicora, L., Towers, G. J., Mechti, N., and Vicenzi, E. (2013) TRIM22 inhibits influenza A virus infection by targeting the viral nucleoprotein for degradation. *J. Virol.* **87,** 4523–4533
43. Gack, M. U., Albrecht, R. A., Urano, T., Inn, K. S., Huang, I. C., Carnero, E., Farzan, M., Inoue, S., Jung, J. U., and Garcia-Sastre, A. (2009) Influenza A virus NS1 targets the ubiquitin ligase TRIM25 to evade recognition by the host viral RNA sensor RIG-I. *Cell. Host Microbe* **5,** 439–449
44. Ohman, T., Rintahaka, J., Kalkkinen, N., Matikainen, S., and Nyman, T. A. (2009) Actin and RIG-I/MAVS signaling components translocate to mitochondria upon influenza A virus infection of human primary macrophages. *J. Immunol.* **182,** 5682–5692
45. Galvan Morales, M. A., Cabello Gutierrez, C., Mejia Nepomuceno, F., Valle Peralta, L., Valencia Maqueda, E., and Manjarrez Zavala, M. E. (2014) Parainfluenza virus type 1 induces epithelial IL-8 production via p38-MAPK signalling. *J. Immunol. Res.* 515984, 2014
46. Zaborowska, J., Baumli, S., Laitem, C., O'Reilly, D., Thomas, P. H., O'Hare, P., and Murphy, S. (2014) Herpes simplex virus 1 (HSV-1) ICP22 protein directly interacts with cyclin-dependent kinase (CDK)9 to inhibit RNA polymerase II transcription elongation. *PLoS ONE* **9**, e107654,
47. Haolong, C., Du, N., Hongchao, T., Yang, Y., Wei, Z., Hua, Z., Wenliang, Z., Lei, S., and Po, T. (2013) Enterovirus 71 VP1 activates calmodulin-dependent protein kinase II and results in the rearrangement of vimentin in human astrocyte cells. *PLoS ONE* **8,** e73900
48. Gee, K., Angel, J. B., Mishra, S., Blahoianu, M. A., and Kumar, A. (2007) IL-10 regulation by HIV-tat in primary human monocytic cells: Involvement of calmodulin/calmodulin-dependent protein kinase-activated p38 MAPK and sp-1 and CREB-1 transcription factors. *J. Immunol.* **178,** 798–807
49. Barnitz, R. A., Wan, F., Tripuraneni, V., Bolton, D. L., and Lenardo, M. J. (2010) Protein kinase A phosphorylation activates vpr-induced cell cycle arrest during human immunodeficiency virus type 1 infection. *J. Virol.* **84,** 6410–6424
50. Li, J., Yu, M., Zheng, W., and Liu, W. (2015) Nucleocytoplasmic shuttling of influenza A virus proteins. *Viruses* **7,** 2668–2682
51. Fujioka, Y., Tsuda, M., Nanbo, A., Hattori, T., Sasaki, J., Sasaki, T., Miyazaki, T., and Ohba, Y. (2013) A ca(2+)-dependent signalling circuit regulates influenza A virus internalization and infection. *Nat. Commun.* **4,** 2763
52. Lakdawala, S. S., Wu, Y., Wawrzusin, P., Kabat, J., Broadbent, A. J., Lamirande, E. W., Fodor, E., Altan-Bonnet, N., Shroff, H., and Subbarao, K. (2014) Influenza a virus assembly intermediates fuse in the cytoplasm. PLoS Pathog. **10,** e1003971
53. Konig, R., Stertz, S., Zhou, Y., Inoue, A., Hoffmann, H. H., Bhattacharyya, S., Alamares, J. G., Tscherne, D. M., Ortigoza, M. B., Liang, Y., Gao, Q., Andrews, S. E., Bandyopadhyay, S., De Jesus, P., Tu, B. P., Pache, L., Shih, C., Orth, A., Bonamy, G., Miraglia, L., Ideker, T., Garcia-Sastre, A., Young, J. A., Palese, P., Shaw, M. L., and Chanda, S. K. (2010) Human host factors required for influenza virus replication. *Nature* **463,** 813–817
54. Khan, K. A., Do, F., Marineau, A., Doyon, P., Clement, J. F., Woodgett, J. R., Doble, B. W., and Servant, M. J. (2015) Fine-tuning of the RIG-I-like Receptor/Interferon regulatory factor 3-dependent antiviral innate immune response by the glycogen synthase kinase 3/beta-catenin pathway. *Mol. Cell. Biol.* **35,** 3029–3043
55. Ludwig, S., Planz, O., Pleschka, S., and Wolff, T. (2003) Influenza-virus-induced signaling cascades: Targets for antiviral therapy? *Trends Mol. Med.* **9,** 46–52
56. Marjuki, H., Gornitzky, A., Marathe, B. M., Ilyushina, N. A., Aldridge, J. R., Desai, G., Webby, R. J., and Webster, R. G. (2011) Influenza A virus-induced early activation of ERK and PI3K mediates V-ATPase-dependent intracellular pH change required for fusion. *Cell. Microbiol.* **13,** 587–601

57. Nacken, W., Anhlan, D., Hrincius, E. R., Mostafa, A., Wolff, T., Sadewasser, A., Pleschka, S., Ehrhardt, C., and Ludwig, S. (2014) Activation of c-jun N-terminal kinase upon influenza A virus (IAV) infection is independent of pathogen-related receptors but dependent on amino acid sequence variations of IAV NS1. *J. Virol.* **88,** 8843–8852
58. Borgeling, Y., Schmolke, M., Viemann, D., Nordhoff, C., Roth, J., and Ludwig, S. (2014) Inhibition of p38 mitogen-activated protein kinase impairs influenza virus-induced primary and secondary host gene responses and protects mice from lethal H5N1 infection. *J. Biol. Chem.* **289,** 13–27
59. Berger, K. L., Cooper, J. D., Heaton, N. S., Yoon, R., Oakland, T. E., Jordan, T. X., Mateu, G., Grakoui, A., and Randall, G. (2009) Roles for endocytic trafficking and phosphatidylinositol 4-kinase III alpha in hepatitis C virus replication. *Proc. Natl. Acad. Sci. U.S.A.* **106,** 7577–7582
60. Jamaluddin, M., Tian, B., Boldogh, I., Garofalo, R. P., and Brasier, A. R. (2009) Respiratory syncytial virus infection induces a reactive oxygen species-MSK1-phospho-ser-276 RelA pathway required for cytokine expression. *J. Virol.* **83,** 10605–10615
61. Karlas, A., Machuy, N., Shin, Y., Pleissner, K. P., Artarini, A., Heuer, D., Becker, D., Khalil, H., Ogilvie, L. A., Hess, S., Maurer, A. P., Muller, E., Wolff, T., Rudel, T., and Meyer, T. F. (2010) Genome-wide RNAi screen identifies human host factors crucial for influenza virus replication. *Nature* **463,** 818–822
62. Hattlmann, C. J., Kelly, J. N., and Barr, S. D. (2012) TRIM22: A diverse and dynamic antiviral protein. *Mol. Biol. Int.* :153415, 2012
63. Gack, M. U., Shin, Y. C., Joo, C. H., Urano, T., Liang, C., Sun, L., Takeuchi, O., Akira, S., Chen, Z., Inoue, S., and Jung, J. U. (2007) TRIM25 RING-finger E3 ubiquitin ligase is essential for RIG-I-mediated antiviral activity. *Nature* **446,** 916–920
64. Zhang, H., Wang, D., Zhong, H., Luo, R., Shang, M., Liu, D., Chen, H., Fang, L., and Xiao, S. (2015) Ubiquitin-specific protease 15 negatively regulates virus-induced type I interferon signaling via catalytically-dependent and -independent mechanisms. *Sci. Rep.* **5,** 11220
65. Zhong, H., Wang, D., Fang, L., Zhang, H., Luo, R., Shang, M., Ouyang, C., Ouyang, H., Chen, H., and Xiao, S. (2013) Ubiquitin-specific proteases 25 negatively regulates virus-induced type I interferon signaling. *PLoS ONE* **8,** e80976
66. Jacobs, J. L., and Coyne, C. B. (2013) Mechanisms of MAVS regulation at the mitochondrial membrane. *J. Mol. Biol.* **425,** 5009–5019
67. Liu, S., Cai, X., Wu, J., Cong, Q., Chen, X., Li, T., Du, F., Ren, J., Wu, Y. T., Grishin, N. V., and Chen, Z. J. (2015) Phosphorylation of innate immune adaptor proteins MAVS, STING, and TRIF induces IRF3 activation. *Science* **347**, aaa2630
68. Hu, J., Rho, H. S., Newman, R. H., Zhang, J., Zhu, H., and Qian, J. (2014) PhosphoNetworks: A database for human phosphorylation networks. *Bioinformatics* **30,** 141–142
69. Berro, R., Pedati, C., Kehn-Hall, K., Wu, W., Klase, Z., Even, Y., Geneviere, A. M., Ammosova, T., Nekhai, S., and Kashanchi, F. (2008) CDK13, a new potential human immunodeficiency virus type 1 inhibitory factor regulating viral mRNA splicing. *J. Virol.* **82,** 7155–7166
70. Bakre, A., Andersen, L. E., Meliopoulos, V., Coleman, K., Yan, X., Brooks, P., Crabtree, J., Tompkins, S. M., and Tripp, R. A. (2013) Identification of host kinase genes required for influenza virus replication and the regulatory role of MicroRNAs. *PLoS ONE* **8,** e66796
71. Munakata, T., Inada, M., Tokunaga, Y., Wakita, T., Kohara, M., and Nomoto, A. (2014) Suppression of hepatitis C virus replication by cyclin-dependent kinase inhibitors. *Antiviral Res.* **108,** 79–87
72. Kapasi, A. J., Clark, C. L., Tran, K., and Spector, D. H. (2009) Recruitment of cdk9 to the immediate-early viral transcriptosomes during human cytomegalovirus infection requires efficient binding to cyclin T1, a threshold level of IE2 86, and active transcription. *J. Virol.* **83,** 5904–5917
73. Kapasi, A. J., and Spector, D. H. (2008) Inhibition of the cyclin-dependent kinases at the beginning of human cytomegalovirus infection specifically alters the levels and localization of the RNA polymerase II carboxyl-terminal domain kinases cdk9 and cdk7 at the viral transcriptosome. *J. Virol.* **82,** 394–407
74. Hutterer, C., Eickhoff, J., Milbradt, J., Korn, K., Zeittrager, I., Bahsi, H., Wagner, S., Zischinsky, G., Wolf, A., Degenhart, C., Unger, A., Baumann, M., Klebl, B., and Marschall, M. (2015) A novel CDK7 inhibitor of the pyrazolotriazine class exerts broad-spectrum antiviral activity at nanomolar concentrations. *Antimicrob. Agents Chemother.* **59,** 2062–2071
75. Wang, D., de la Fuente, C., Deng, L., Wang, L., Zilberman, I., Eadie, C., Healey, M., Stein, D., Denny, T., Harrison, L. E., Meijer, L., and Kashanchi, F. (2001) Inhibition of human immunodeficiency virus type 1 transcription by chemical cyclin-dependent kinase inhibitors. *J. Virol.* **75,** 7266–7279
76. Pauls, E., Badia, R., Torres-Torronteras, J., Ruiz, A., Permanyer, M., Riveira-Munoz, E., Clotet, B., Marti, R., Ballana, E., and Este, J. A. (2014) Palbociclib, a selective inhibitor of cyclin-dependent kinase4/6, blocks HIV-1 reverse transcription through the control of sterile alpha motif and HD domain-containing protein-1 activity. *AIDS.* **28,** 2213–2222
77. Breuer, D., Kotelkin, A., Ammosova, T., Kumari, N., Ivanov, A., Ilatovskiy, A. V., Beullens, M., Roane, P. R., Bollen, M., Petukhov, M. G., Kashanchi, F., and Nekhai, S. (2012) CDK2 regulates HIV-1 transcription by phosphorylation of CDK9 on serine 90. *Retrovirology* **9**, 94-4690-9-94
78. Kudoh, A., Daikoku, T., Sugaya, Y., Isomura, H., Fujita, M., Kiyono, T., Nishiyama, Y., and Tsurumi, T. (2004) Inhibition of S-phase cyclin-dependent kinase activity blocks expression of epstein-barr virus immediate-early and early genes, preventing viral lytic replication. *J. Virol.* **78,** 104–115
79. Holcakova, J., Tomasec, P., Bugert, J. J., Wang, E. C., Wilkinson, G. W., Hrstka, R., Krystof, V., Strnad, M., and Vojtesek, B. (2010) The inhibitor of cyclin-dependent kinases, olomoucine II, exhibits potent antiviral properties. *Antivir. Chem. Chemother.* **20,** 133–142
80. Tong, W. G., Chen, R., Plunkett, W., Siegel, D., Sinha, R., Harvey, R. D., Badros, A. Z., Popplewell, L., Coutre, S., Fox, J. A., Mahadocon, K., Chen, T., Kegley, P., Hoch, U., and Wierda, W. G. (2010) Phase I and pharmacologic study of SNS-032, a potent and selective Cdk2, 7, and 9 inhibitor, in patients with advanced chronic lymphocytic leukemia and multiple myeloma. *J. Clin. Oncol.* **28,** 3015–3022
81. Blachly, J. S., and Byrd, J. C. (2013) Emerging drug profile: Cyclin-dependent kinase inhibitors. *Leuk. Lymphoma* **54,** 2133–2143
82. Wathelet, M. G., Lin, C. H., Parekh, B. S., Ronco, L. V., Howley, P. M., and Maniatis, T. (1998) Virus infection induces the assembly of coordinately activated transcription factors on the IFN-beta enhancer in vivo. *Mol. Cell* **1,** 507–518
83. Rintahaka, J., Wiik, D., Kovanen, P. E., Alenius, H., and Matikainen, S. (2008) Cytosolic antiviral RNA recognition pathway activates caspases 1 and 3. *J. Immunol.* **180,** 1749–1757
84. Nencioni, L., De Chiara, G., Sgarbanti, R., Amatore, D., Aquilano, K., Marcocci, M. E., Serafino, A., Torcia, M., Cozzolino, F., Ciriolo, M. R., Garaci, E., and Palamara, A. T. (2009) Bcl-2 expression and p38MAPK activity in cells infected with influenza A virus: Impact on virally induced apoptosis and viral replication. *J. Biol. Chem.* **284,** 16004–16015
85. Kakkola, L., Denisova, O. V., Tynell, J., Viiliainen, J., Ysenbaert, T., Matos, R. C., Nagaraj, A., Ohman, T., Kuivanen, S., Paavilainen, H., Feng, L., Yadav, B., Julkunen, I., Vapalahti, O., Hukkanen, V., Stenman, J., Aittokallio, T., Verschuren, E. W., Ojala, P. M., Nyman, T., Saelens, X., Dzeyk, K., and Kainov, D. E. (2013) Anticancer compound ABT-263 accelerates apoptosis in virus-infected cells and imbalances cytokine production and lowers survival rates of infected mice. *Cell. Death Dis.* **4,** e742
86. Li, H. X., Zhao, W., Shi, Y., Li, Y. N., Zhang, L. S., Zhang, H. Q., and Wang, D. (2015) Retinoic acid amide inhibits JAK/STAT pathway in lung cancer which leads to apoptosis. *Tumour Biol.* **36,** 8671–8678
87. Thomas, P. G., Dash, P., Aldridge JRJr, Ellebedy, A. H., Reynolds, C., Funk, A. J., Martin, W. J., Lamkanfi, M., Webby, R. J., Boyd, K. L., Doherty, P. C., and Kanneganti, T. D. (2009) The intracellular sensor NLRP3 mediates key innate and healing responses to influenza A virus via the regulation of caspase-1. *Immunity* **30,** 566–575
88. Ichinohe, T., Pang, I. K., and Iwasaki, A. (2010) Influenza virus activates inflammasomes via its intracellular M2 ion channel. *Nat. Immunol.* **11,** 404–410
89. Nain, M., Hinder, F., Gong, J. H., Schmidt, A., Bender, A., Sprenger, H., and Gemsa, D. (1990) Tumor necrosis factor-alpha production of influenza A virus-infected macrophages and potentiating effect of lipopolysaccharides. *J. Immunol.* **145,** 1921–1928